IBRACON Structures and Materials Journal
Revista IBRACON de Estruturas e Materiais
ISSN 1983-4195 ismj.org

REVIEW

Reaction mechanisms of alkali-activated materials

Mecanismos de reação de materiais álcali ativados

Markssuel Teixeira Marvila[a]
Afonso Rangel Garcez de Azevedo[a]
Carlos Maurício Fontes Vieira[a]

[a]Universidade Estadual do Norte Fluminense – UENF, Laboratório de Materiais Avançados – LAMAV, Campos dos Goytacazes, RJ, Brasil

Received 17 April 2020
Accepted 28 October 2020

Abstract: The Alkali-Activated Materials (AAM) are defined as materials obtained through the reaction between precursors and activators, and are separated into two classes depending on the products formed in the reaction, those rich in calcium, as the blast furnace slag, whose Ca/(Si+Al) ratio is higher than 1; and poor in calcium, which is the geopolymers subclass. In this review article, some bibliographical aspects were discussed regarding the discovery of these materials, through research conducted by Victor Glukhovsky and through the characterization of historical monuments by Davidovits, which began in the 50s and 60s and persist to the present day. The main products obtained in the alkaline activation reaction were also addressed, using the definition of polysialates and zeolites, in the case of geopolymers, and the tobermorite structure, in the case of materials rich in calcium. The main steps of the alkali-activated reaction, such as dissolution, condensation, polycondensation, crystallization, and hardening, were discussed. Some techniques for characterizing the AA reaction products were also examined, such as X-ray diffraction (XRD), nuclear magnetic resonance spectrometry (NMR), Fourier transform infrared spectroscopy (FTIR), and scanning electron microscopy (SEM). Finally, the main factors that interfere in the kinetics of AA reactions were explored, in which the type of cure and the activating solution used in the alkali-activated materials production stands out.

Keywords: alkali-activated materials, geopolymers, precursors.

Resumo: Os materiais álcali ativados (MAA) são definidos como materiais obtidos por intermédio da reação entre precursores e ativadores, e são separados em duas classes dependendo dos produtos formados na reação, os ricos em cálcio, como é o caso da escória de alto forno, cuja relação Ca/(Si+Al) é maior do que 1; e pobres em cálcio, que constitui a subclasse dos geopolímeros. Nesse artigo de revisão foram discutidos alguns aspectos bibliográficos a respeito da descoberta desses materiais, por meio de pesquisas realizadas por Victor Glukhovsky e por meio da caracterização de monumentos históricos por Davidovits, que se iniciaram nas décadas de 50 e 60 e persistem até os dias atuais. Também foram abordados os principais produtos obtidos na reação de ativação alcalina, utilizando a definição de polissialatos e zeólitas, no caso dos geopolímeros, e da estrutura da tobermorita, no caso dos materiais ricos em cálcio. As principais etapas da reação álcali ativadas, como dissolução, condensação, policondensação, cristalização e endurecimento, foram debatidas. Algumas técnicas para caracterização dos produtos da reação AA também foram examinadas, tais como difração de raios-X (DRX), espectrometria de ressonância magnética nuclear (RMN), espectroscopia no infravermelho com transformada de Fourier (FTIR) e microscopia eletrônica de varredura (MEV). Por fim, foram explorados os principais fatores que interferem na cinética das reações AA, onde destaca-se o tipo de cura e de solução ativadora utilizada na produção dos MAA.

Palavras-chave: materiais álcali ativados, geopolímeros, precursores.

How to cite: M. T. Marvila, A. R. G. Azevedo, and C. M. F. Vieira, "Reaction mechanisms of alkali-activated materials," *Rev. IBRACON Estrut. Mater*., vol. 14, no. 3, e14309, 2021, https://doi.org/10.1590/S1983-41952021000300009

Corresponding author: Markssuel Teixeira Marvila. E-mail: markssuel@hotmail.com
Financial support: CNPq, proc. nº 301634/2018.1; FAPERJ, proc. nº E-26/202.773/2017.
Conflict of interest: Nothing to declare.

1 INTRODUCTION

1.1 Alkali -activated materials definition

Alkali-activated materials (AAM) are obtained from two basic components, the activator, and the precursor. The material used as a precursor is usually in powdered and mineralogically amorphous form. It can be composed of aluminum silicates, and they are named geopolymers, or present in its composition a predominance of calcium oxide [1], as occurs with blast furnace slag (BFS). The activating materials, in turn, are composed of alkali metals, in the form of hydroxide or silicates, dissolved in an aqueous solution. They are responsible for causing the hardening reactions due to high alkalinity, manifested by the high pH, above 14 [2]

1.2 Historical aspects

Historically alkali-activated materials were developed by Victor Glukhovsky in the 1950s and 1960s in the Soviet Union. The researcher developed systems activated in an alkaline manner by mixing materials from volcanic processes (rocks and ash) with activating solutions based on sodium hydroxide. In response, he obtained materials with a composition similar to Portland cement after hardening, that is, hydrated calcium silicate phases (C-S-H) [3]. These materials were named as soil silicates.

Around 1979, Davidovits, a French researcher and chemist, developed an Alkali-activated material using natural origin materials rich in silicon and aluminum, such as kaolin clay, activated by the solution of alkaline liquids [4]. The researcher patented his discovery by naming the materials obtained as geopolymers since they are obtained by a polymerization reaction similar to the one that gives rise to polymeric materials. However, unlike polymers, geopolymers have an inorganic composition. Because of this, another appropriate definition for these materials is that they are called inorganic polymers [5].

Although only the contributions of Victor Glukhovsky and Davidovits were highlighted, other researchers contributed considerably to the knowledge of AAM. Table 1 presents the main contributions of several researchers to the development of alkali activation reaction science. It is observed that initially, the researchers were concerned with characterizing building materials extracted from ancient monuments, such as the Roman aqueducts studied by Malinowski in 1979 and the Egyptian pyramids studied by Davidovits, and Sawyer in 1985 [6]. The authors proved that the materials used in these important monuments were obtained through alkaline activation processes. This fact motivated more researches in this area, and other alkaline activation studies carried out by Roy et al. (1991), Palomo and Glasser (1992) and Krivenko (1994), who, despite obtaining important results, still could not fully explain the mechanisms of alkali-activated reactions [6].

In 1994, Davidovits [7] presented a complex analysis on the microstructure of geopolymers through polysialate networks, and in 1995 Wang and Scrivener presented microstructural analyzes of alkali-activated materials rich in calcium [6]. These surveys improved the researchers' understanding of alkali-activated materials. In 2007, Provis and Van Deventer [8] presented a kinetic model of geopolymerization reactions using X-ray diffraction techniques that were able to explain the stages of this reaction by correlating them with the morphological structure of the gels formed.

In 2011, Habert et al. [9] carried out the environmental evaluation of the geopolymer concrete production by analyzing the life cycle, comparing it with the production cycle of Portland cement. The authors proved the environmental importance of the study of the alkali-activated material, which was shown as an ecological alternative to conventional Portland cement concrete.

After the consolidation of the main concepts related to the alkali-activated materials science, the material started to be used in larger constructions. As an example, we can mention the Australian constructions of the Victoria bridge in 2013 and the expansion of Brisbane West Wellcamp airport in 2014 with E-Creta, an alkali-activated concrete [10].

Recently, Davidovits developed research characterizing the material present in ancient monuments of pre-Columbian civilizations in South America, concluding that they were alkali-activated materials [11]. The studies carried out between 2016 and 2019 in the Tiahuanaco monuments (Tiwanaku/Pumapunku), Bolivia, and other monuments in Peru complement the studies carried out in the 70s and 80s and prove the durability of alkali-activated materials [12].

Table 1. Bibliographic history of some important discoveries about activated alkali materials. Source [6]–[12]:

Author	Year	Research
Feret	1939	Use of slag in cement
Purdon	1940	Combination of slag and alkaline solutions
Glukhovsky	1959	Theoretical basis and development of alkaline solutions in cement
Glukhovsky	1965	First material called alkaline cement
Davidovits	1979	Use of the term geopolymer
Malinowski	1979	Characterization of ancient Roman aqueducts
Forss	1983	Cement with alkaline slag and superplasticizers
Langton e Roy	1984	Characterization of old building materials
Davidovits e Sawyer	1985	Patent of a cement with chemical composition similar to the material that it believes to have been used in Egyptian pyramids
Krivenko	1986	Definition of M_2O-MO-SiO_2-H_2O
Malolepsy e Petri	1986	Activation of synthetic slags
Malek. et al.	1986	Application of radioactive waste in activated slag cements
Davidovits	1987	Comparison of old and modern cements
Deja e Malolepsy	1989	Proof of chloride resistance of AA materials
Kaushal et al.	1989	Incorporation of nuclear waste in AA materials
Roy e Langton	1989	Concrete production similar to the old ones
Majundar et al.	1989	$C_{12}A_7$ - slag activation
Talling e Brandstetr	1989	Alkaline slag activation
Wu et al.	1990	Alkaline activation of slag-based cement
Roy et al.	1991	Production of quick-setting alkaline cements
Roy e Silsbee	1992	Publication of the article “Alkaline activated cements: an overview”
Palomo e Glasser	1992	Activation of metakaolin
Krivenko	1994	Properties of alkaline cements
Davidovits	1994	Definition of the structure of geopolymers through polysialates
Wang e Scrivener	1995	Discovery of the microstructure of AA materials
Palomo	1999	Publication of the article “Alkaline activation of fly ash: the cement of the future”.
Krivenko, Roy e Shi	2006	Publication of the first book on alkaline activation
Provis e Deventer	2007	Definition of the kinetic modeling of the alkaline activation reaction
Habert et. al	2011	Environmental assessment of geopolymeric concrete production by life cycle
Australia	2013	Construction of the bridge in Victoria with E-Crete.
Australia	2014	Brisbane West Wellcamp airport expansion with E-Crete.
Davidovits	2016	Studies of deposits and monuments used by pre-Columbian civilizations in Bolivia and Peru
Davidovits	2019	Characterization of pre-Columbian monuments in Pumapunku-Tiwanaku, Bolivia

1.3 Advantages and disadvantages

As noted by the main invocations highlighted in the text and Table 1, research involving alkali-activated materials has gained considerable prominence in the construction materials scenario. Provis [2] highlights that this interest in the development of alkali-activated binders is motivated by economic advantages since the process allows the use of industrial by-products, such as slag and ash, to produce a material with considerable added value, which rivals with Portland cement. Another issue pointed out by Provis to explain why the increase in research is linked to sustainable development. It is known that the Portland cement production is very exploratory, besides emitting several tons of CO_2 into the environment. This fact is not repeated in the cycle for the production of alkali-activated materials due to the

possibility of using by-products from other processes, which would be generated regardless of their application as a precursor to AAM.

In addition to those mentioned, different motivations for the development of more research on alkali-activated binders are related to the properties that these materials have. High chemical resistance to acids and high-temperature resistance is mentioned, due to the presence of alkaline aluminosilicate gels, with a highly reticulated nature, in addition to the low presence of water in their structure, when compared to hydrated Portland cement, which presents hydrated calcium silicate gels [13], [14]. AAM can also have good durability and high initial resistance, mainly in slag-based compounds [6]. They also have low shrinkage, low thermal conductivity, strong adhesion to metallic and non-metallic substrates [15], low permeability to ions and chlorides, low cost, a possibility to recover industrial waste, low CO2 emissions, effective passivation of reinforcing steel, making it possible to be armed, if necessary [14].

Although the researchers do not deal much with the subject, the main disadvantages to be overcome for the application of AAM are related to the activating solution, due to two aspects: the difficulty of handling this material, which because it has a very high pH and it is very alkaline it can cause burns or respiratory problems when inhaling the hydroxides dust used in the solution; and the cost and availability of the silicates and hydroxides used in the solution. There are currently few studies on the use of waste as activators in AAM. The vast majority of researchers focus their studies on the development of new precursors. One of the major disadvantages of alkali-activated materials is linked to activators, which still use commercial materials, causing the exploitation of natural resources and making the price of the materials go up. It is noteworthy that the use of alternative activators tends to reduce these disadvantages, although in some cases there is a need for additional treatments, besides those carried out in commercial products, to make them suitable for use. This fact can cause an increase in the price of alternative activators, as highlighted by Azevedo et al. [16], who studied the application of glass waste in place of sodium silicate. The authors concluded that it is necessary to grind the residue for a long time, consuming a considerable amount of energy in the process.

1.4 Alkali-activated materials classification

To organize the structure of this study, the explanation of the alkaline activation mechanisms, the principal objective of this article, will be divided into two groups, as suggested by some authors [17], [18]:

a) Materials with precursors rich in aluminosilicates and without calcium oxide in their composition, such as metakaolin and ashes. These materials were the focus of Davidovits' study, and when they suffer the reaction, it becomes a mineralogical structure very similar to zeolites, as will be discussed below. They are known as geopolymers, geocements or polysialates [6].

b) Materials with precursors rich in calcium oxide, which may have aluminum oxide or not. They are precursors that have a Ca/(Si+Al) ratio higher than 1 [1]. They were the focus of study by Victor Glukhovsky, and when they harden, they present a composition similar to ordinary Portland cement, that is, they form C-S-H gels [19], [20].

2 ALKALI ACTIVATION REACTION OF LOW-CALCIUM PRECURSORS

2.1 Main low-calcium precursors

The main precursors used in alkaline activation for the geopolymers production, that is, the low-calcium precursors content are metakaolin and fly ash. Regarding metakaolin, it is worth noting that this compound has several studies carried out and it is considered by researchers as the principal material used as a precursor in AA reactions [21], [22]. The significant use of metakaolin can be attributed to its reactivity, which is quite high [23], and the way of obtaining the material, which is very simple.

This material is generated by calcining kaolin at temperatures ranging from 500 to 800ºC, depending on the degree of crystallization and the purity of the material [24]. It is known that kaolinite, which is the main compound present in kaolin, undergoes a dehydroxylation reaction at around 550ºC, transforming into metakaolinite. Figure 1 shows a scheme for the production of metakaolin from traditional kaolin [1], [20], [25]. It is observed that the burning at temperatures below 400ºC is not suitable for the precursor production, as well as the burning of temperatures above 950ºC, due to the mullite production that cannot be activated alkali due to its high crystallinity [15], [19].

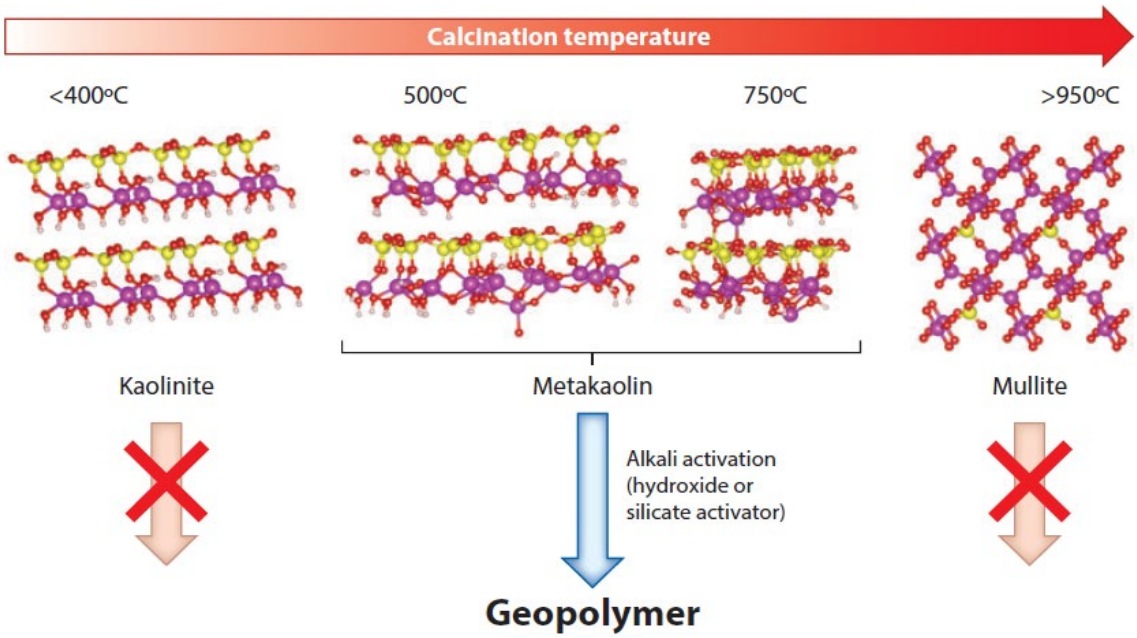

Figure 1. Calcination of kaolin for percussion production. Source: White et al. [20].

On environmental issues, it is interesting to note that there are some advantages in using metakaolin because its synthesis emits 5 to 6 times less CO_2 than the Portland cement production process [26]. Besides, kaolin can be extracted not only from mineral sources but depending on the composition, it can be obtained through mine tailings or the paper industry [1]. The different sources will influence the reactivity of the obtained metakaolin, depending on, for example, the chemical and mineralogical composition of the clay used as raw material, but they are more ecologically viable solutions.

As for the disadvantages of the metakaolin use, we can mention a higher tendency of drying retraction presented by these materials when compared to fly ash [27]. This characteristic can be related to the chemical composition of these two precursors, which it is observed that metakaolin has a higher amount of aluminum oxide (Al_2O_3) than fly ash. Overall, some research shows that metakaolin has about 55 to 62% SiO_2 and between 35 to 42% Al_2O_3, while fly ash has between 50 to 55% SiO_2 and approximately 20 to 25% Al_2O_3 [24], [28]–[30]. The retraction is higher because the aluminum oxide dissolves faster than the silicon oxide, related to the two principal network makers in geopolymers [24]. That also explains the reactivity of metakaolin being higher than fly ash.

Another disadvantage is the price of metakaolin, which, because it is a commercial material, is usually higher than when using blast furnace slag, fly ash, or other industrial waste [15]. However, it is noteworthy that the price of metakaolin is extremely variable, depending on the location and specifications of the product, for example. Thus, even though there is a tendency for the price of metakaolin to be higher than in the other components used as precursors, commonly residues, this statement cannot be generalized. However, due to the high purity and reactivity, the products obtained by the alkaline reaction of metakaolin, in general, present a more well-defined gel microstructure [1].

On fly ash, it is worth noting that this material is a powdered by-product produced in thermoelectric plants during the coal burning, containing mainly aluminosilicate. They present fine spherical particles with the main chemical components of aluminum, silicon, calcium, iron, magnesium, and carbon wastes [31]. The particle size in the fly ash ranges from <1 μm to more than 100 μm, and this by-product has an annual worldwide production of more than 900 million tons, according to the updated data from 2019 [15]. Therefore, the storage and fly ash disposal as industrial waste has become a serious environmental problem and a worldwide technical challenge. In Brazil, however, the energy matrix uses predominantly hydroelectric plants, which do not generate fly ash. For this reason, the study of this type of waste in Brazilian research is less practical, different from what occurs in other countries, such as China and the USA, which present easy availability of the waste [32].

Given its low price, good spherical structure, and a large amount of highly active amorphous aluminates and silicates, fly ash class F is the most recommended raw material for geopolymers synthesis [33]. The activity and solubility of Al

and Si can transform precursors into important geopolymeric products in an alkaline activator solution [34], [35]. According to the American Society of Test Materials classification [34], fly ash is defined as Class C (CaO> 20%) and Class F fly ash (CaO <20%), respectively. Class C fly ash can be hydrated to form hydrated calcium silicate (CSH), has been widely used to partially replace cement in concrete, or as a calcium-rich precursor [31], [35], which will be discussed next in the explanation about AA of BFS. Class F fly ash is more suitable for geopolymers synthesis [36] because its amorphous content is higher than that one of class C fly ash [37].

The geopolymer products obtained with the use of Class F fly ash have excellent mechanical properties, as reported by the literature [35], [38]–[40]. The authors, however, report difficulty in the geopolymers synthesis with fly ash due to the curing of the material that must be done at high temperatures to increase the reactivity of the material, which is very low at ambient temperatures. This characteristic can be associated with the fly ash chemical composition, which, due to its higher levels of Al_2O_3,, as reported [24], [28]–[30], and, in some specific cases, may have a high CaO content, around 12% [41], [42], justifying the need for thermal curing.

Besides metakaolin and fly ash, other types of precursors that have low amounts of calcium have reaction mechanisms typical of geopolymers. For example, other types of burnt clay can be cited as illite-smectites [43] or feldspars [44], [45]. There are also other precursors such as volcanic ash, natural pozzolans, and metallurgical slags with low amounts of calcium [46]–[49]. Recent research has proposed the application of industrial wastes, such as chamotte [50], from ceramics industries, and magnesium phosphate, from the chemical industry through ammonium production [51]. In both cases, there was a potential for the application of waste, but not in isolation. In the case of chamotte, the best results were obtained using 50% metakaolin and 50% waste [50], while in the case of magnesium phosphate, the most satisfactory results were obtained using 30% metakaolin and 70% waste, in which the authors obtained compressive strength of 30 MPa with only 7 hours of curing [51].

2.2 Stages of the alkaline activation reaction of geopolymers

According to Duxson et al. [52], in geopolymers, the alkaline activation reaction is divided, in general, into the following steps: dissolution, condensation, polycondensation, and crystallization of the gels. These steps constitute the Davidovits model, outlined by Duxson, and are briefly explained below, according to the scheme represented by Figure 2.

The first reaction process is the dissolution of the aluminosilicate materials and the release of the reactive monomers silicate and aluminate, represented respectively by $[Si(OH)_4]^-$ and $[Al(OH)_4]^-$. Dissolution occurs by dropping the covalent bonds Si-O-Si and Al-O-Al that characterize aluminosilicates and is only possible in the presence of a strongly alkaline medium with a pH higher than 14, provided by the activating solution. More simply, it can be said that the alkaline solution breaks the bonds that hold aluminosilicates together, creating a colloidal phase [15], [52], [53].

The colloidal phase initiates a water elimination process, due to a nucleophilic substitution reaction, where the specimens $[Si(OH)_4]^-$ and $[Al(OH)_4]^-$, which present an electric charge -1, are connected to the others due to the attraction among the OH groups of the silicate with the Al ions of the aluminates. The colloidal phases initiate the chemical equilibrium process, which is known as condensation, giving rise to intermediate compounds. In this stage, the formation of an unstable aluminosilicate species occurs, releasing water molecules in the process [14], [53].

This procedure continues, with more water release and the first gels formation. The search for balance continues, however, load balancing is not possible, because both aluminates and silicates have negative charges. Because of this, the presence of alkali metal ions, such as Na^+ ou K^+, in the alkaline solution is so important. The positive charge of these ions provides a balance in the charges of the unstable gels that had been formed, causing a reorganization in the structure of the intermediate compounds, which initiate the formation of a more resistant final compound.

The polycondensation of the gels then occurs, which may or may not undergo crystallization and give rise to the stable gels present in the geopolymers final structure. Amorphous gels are called by some authors N-A-S-H (hydrated sodium aluminosilicate), while the crystalline or semi-crystalline phases are just called zeolites [54]. The material starts the hardening process, acquiring mechanical resistance and the other known properties of these activated alkali materials [15], [53]. Figure 3 shows the final structure of the 3D network formed in the composition of the geopolymers.

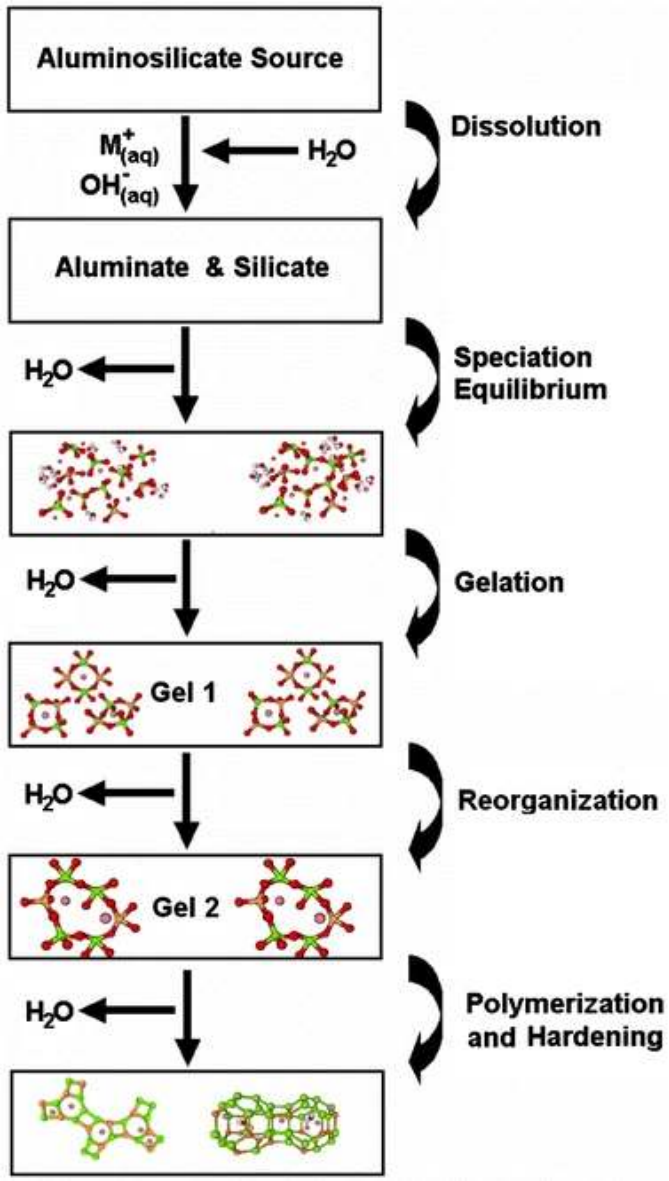

Figure 2. Duxson model of alkaline activation reaction of geopolymers (low in calcium). Source: Duxson et al. [53].

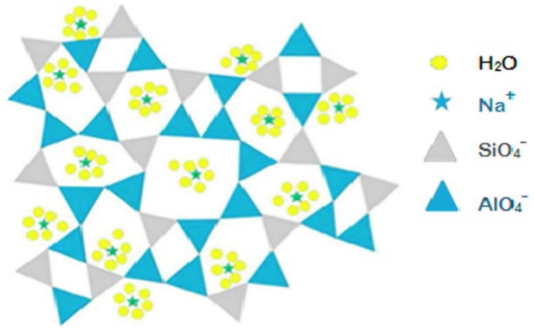

Figure 3. Illustration of the geopolymeric network in formation, amorphous N-A-S-H gels. Source: Lahoti et al. [14].

2.3 Compounds formed in the alkaline activation reaction of geopolymers

As mentioned above, some authors point out that the geopolymers formation follows a logic very similar to the zeolites formation, and this characteristic is addressed in the sequence of this text [14], [15], [52], [53]. What is worth noting is that the geopolymerization reactions give rise to polysialate compounds, which can have different configurations, depending on how the alkaline activation reaction is processed [7], [55].

The polysialate compounds correspond to three-dimensional networks of SiO_4 and AlO_4 tetrahedrons sharing the oxygen atoms, as shown in Figure 3. To maintain balance, the existence of positive Na^+, K^+ e Ca^{2+} ions is necessary, which must be present in the structure cavities to balance the negative charges of geopolymeric gels. Polysialates can also be defined as chain and ring polymers with Si^{4+} and Al^{3+} in coordination 4 times with oxygen, and their empirical formula is given by the equation below [3].

$$M_n\left[-\left(Si-O_2\right)_z-Al-O\right]_n.wH_2O \tag{1}$$

Where z=1, 2 or 3, represents the atomic relationship between Si/Al; M= monovalent cation as K^+ ou Na^+; n= geopolymerization degree.

The types of polysialates distinguished by Davidovits are illustrated in Figure 4, being differentiated according to the atomic relationship between Si/Al [6] or between the molar ratio of SiO_2/Al_2O_3 [5], depending on the studied author. It is worth noting that the atomic relationship between Si/Al is half the molar ratio between SiO_2/Al_2O_3. For example, when the atomic ratio is 1, the molar ratio is 2, and so on.

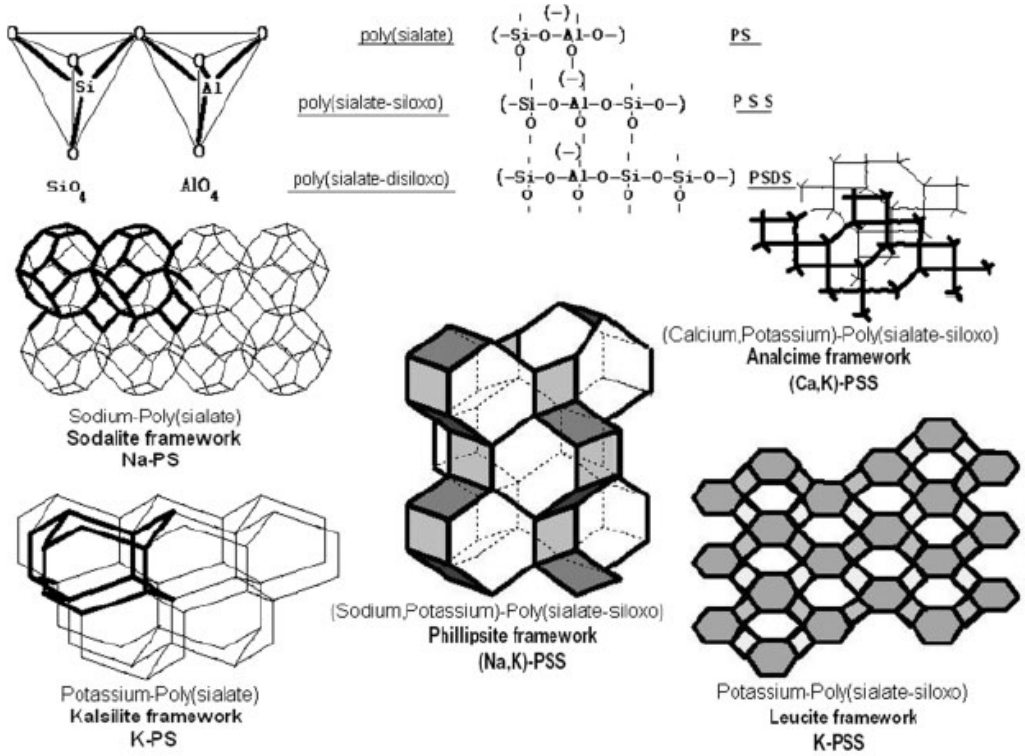

Figure 4. Geopolymer networks of Polysialates. Source: Majidi [5].

Taking the molar ratio as a base, we have the following classification: common polysialates (PS), where the SiO_2/Al_2O_3 ratio is 2, forming a type structure (Si - O - Al - O); polysialates-siloxo (PSS), with a SiO_2/Al_2O_3ratio of approximately 4 and (Si - O - Al - O - Si - O) structure; and polysialates-disiloxo (PSDS), with a molar ratio of SiO_2/Al_2O_3 around 6 and chains of the type (Si - O - Al - O - Si - O - Si - O). This information can be seen in Figure 4,

where the networks of PS and PSS formed with the alkali metals sodium and potassium are visualized, such as the networks of kalsilite, leucilite, analcime, sodalite. The formation of these networks is directly related to the dosage of geopolymers in their production phase, either through molar relationships, solution molarity, or in the relationship between the activator and the precursor.

It is worth noting that, besides the model proposed by Davidovits for the geopolymerization reaction, there is another model that is very widespread and accepted in the study of this material, which is the Provis model [56]. In this model, detailed in Figure 5, it is defined that the precursor reaction rich in aluminosilicates and poor in calcium oxide, as in the case of metakaolin and fly ash, occurs initially with the formation of silicate and aluminate monomers, which grouped forming combined aluminosilicate oligomers. Thereafter, the reaction "separates" into two stages, in which part of the oligomers polymerizes in an amorphous and random manner, giving rise to geopolymeric gels. The other part undergoes the process of crystalline nucleation, forming nanocrystalline aluminosilicates nuclei, which subsequently originates crystalline zeolite phases. According to the Provis model, two distinct and simultaneous geopolymer formation reactions occur to a higher or lesser degree depending on different factors (such as temperature, cure time, solution's molarity, and molar relationships of the precursors), originating an amorphous phase and another crystalline [8], [57].

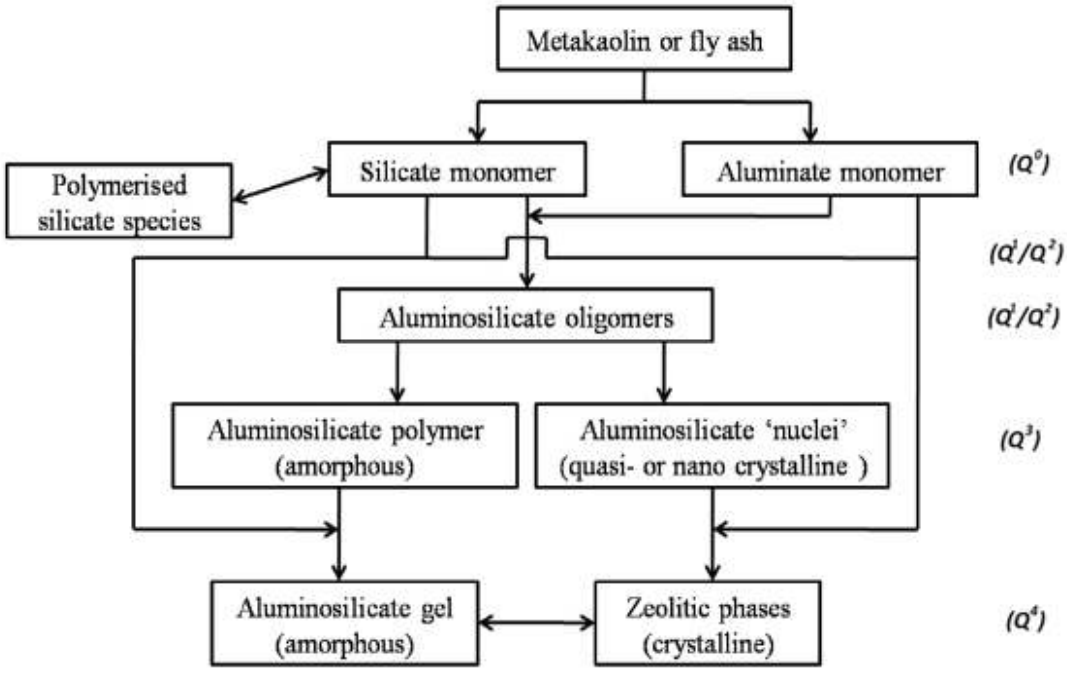

Figure 5. Provis model for the formation of geopolymers. Source: Wu [15].

The mechanism of polysialates formation, and also of the zeolite phases, is much more complex than was mentioned above. It is known, for example, that in the alkaline activation reaction of geopolymers, the polysialates formation formed mainly by iron oxide can occur, named as ferrosialates [58]. Iron can be present in three different forms in the ferrosalate chain: in Fe^{+3} species trapped in the main chain, in Fe^{+3} species acting for load balancing in interstitial sites or in the form of Fe_3O_4 oxide linked to the chain through bonds secondary [59]. In general, iron forms a $[Fe(OH)]^{2+}$ specimen that replaces $[Al(OH)_4]^-$ specimens. In some cases it can also partially replace specimens $[Si(OH)_4]^-$ in the geopolymer chain [58].

These compounds promote tensile strength in the geopolymer, which in general is low, but make the material conducive to the occurrence of corrosion, which in the case of use in conjunction with reinforced elements, may make the application of the material unfeasible [60]. Another property presented by ferrosialates is the of the geopolymer density reduction, due to its lamellar, tubular and spongy structure. This characteristic, however, increases the porosity of geopolymers with a high content of ferrosialates [59].

Although the formation of ferrosialates is benefited in precursors that have a high amount of iron oxide and whose cure is carried out at temperatures above 80ºC, practically all geopolymers have low amounts of ferrosialates in their composition [61]. This fact illustrates and proves the complexity of the polysialate networks formation, which although simplified by several authors, presents mechanisms that are still little explored.

Figure 5 presents the information for Q^n, where n can take values from 1 to 4. This notation represents the silicon tetrahedral atom coordination, connected via oxygen to other silicon tetrahedral atoms [25]. It is possible to notice that as the geopolymerization reaction becomes more intense, larger amounts of chains are formed, the silicon tetrahedrons coordination increases, which bind and form gels. This analysis is performed by specific techniques such as nuclear magnetic resonance spectrometry, where it is possible to obtain the Q^n which means the silicon atoms quantity covalently linked.

It is noticed that the zeolites formation is a common characteristic and highlighted by different authors. That is why it will be explained what zeolites are and what their similarities are with geopolymers. Zeolites are hydrated, crystalline, or nanocrystalline aluminosilicates with a specific structure, composed of silica and alumina tetrahedra connected by shared oxygen atoms and containing well-defined channels and chambers, filled with ions and water molecules [54]. This structure makes its physical and chemical properties unique, which results in a wide range of practical applications [25]. The zeolites are based on the tetrahedron TO_4, where T is an aluminum or silicon atom, which can be considered as a basic building block. The connections between several TO_4 tetrahedrons are called secondary units of construction (USF) [40].

The main difference between conventional zeolites and those formed in geopolymerization is that, in conventional production the molar ratios are much higher. For example, while in conventional production the molar ratio between H_2O/SiO_2 is between 10 and 100 and the molar ratio between OH^-/SiO_2 is between 2 and 20, in the case of geopolymers these relationships change to between 2 and 10 and between 0.1 and 0.5, respectively [62]. As an impact on the standard zeolites formation, a high crystallinity content is achieved, while in the formation of geopolymers zeolites are not formed separately, but they are mixed with amorphous gels of the N-A-S-H type, leading to more amorphous compounds [40]. In the case of geopolymers, a kind of composite material is formed and it has two distinct phases: a crystalline one formed by zeolites and an amorphous one, formed mainly by N-A-S-H gels.

Even if the geopolymerization reaction forms zeolites are not as pure as in the conventional process, which occurs by autoclave requiring a specific hydrothermal reactor, there is a great energy advantage in the geopolymerization process. The geopolymerization reaction, in addition to saving energy, provides time spent, contributing to sustainability in obtaining zeolites [54]. However, it is worth noting that zeolites are formed only in very specific situations within geopolymers, under predetermined temperatures (25 to 300ºC) and pressure [63], [64].

The most commonly known zeolite species are analcime, zeolite A, zeolite X, sodalite, natrolite, among others [54], [65], highlighted in Table 2. As can be seen in Figure 4, some zeolite minerals are the same detailed in this figure as geopolymerization reaction products. The polysialates highlighted above are nothing more than zeolites with a lower degree of crystallinity due to the presence of amorphous N-A-S-H gels. Figure 6 presents an illustration of the sodalite-type zeolites (SOD), zeolite A (LTA), and zeolite X (FAU), which are formed by the arrangement of sodalite cages in different configurations. This fact illustrates that the most common zeolites obtained by the autoclave process are formed in geopolymers, but the simplest crystallographic arrangements, which favor the formation of larger amounts of sodalite as a result of zeolite A or X [65].

Table 2. Parameters of the main zeolites. Source: Rożek et al. [54]:

Abbreviation	Name	Chemical formula
ANA	analcime	$Na[AlSi_2O_6].H_2O$
CAN	hydroxycancrinite	$Na_8[AlSiO_4]_6(OH)_2.2H_2O$
CHA	chabazite (herschelite)	$Na[AlSi_2O_6].3H_2O$
FAU	Faujasite (Zeolite X)	$Na_2[Al_2Si_2.4O_{8,8}].6,7H_2O$
FAU	Faujasite (Zeolite Y)	$Na_{1.88}[Al_2Si_{4,8}O_{13,54}].9H_2O$
GIS	Zeolite Na-P1	$Na_{3,6}[Al_{3,6}Si_{12,4}O_{32}].12\ H_2O$
LTA	Zeolite A	$Na_2[Al_2Si_{1,85}O_{7,7}].5\ H_2O$
NAT	Natrolite	$Na_2[Al_2Si_3O_8].2\ H_2O$
SOD	Sodalita	$Na_6[AlSiO_4]_6.8\ H_2O$

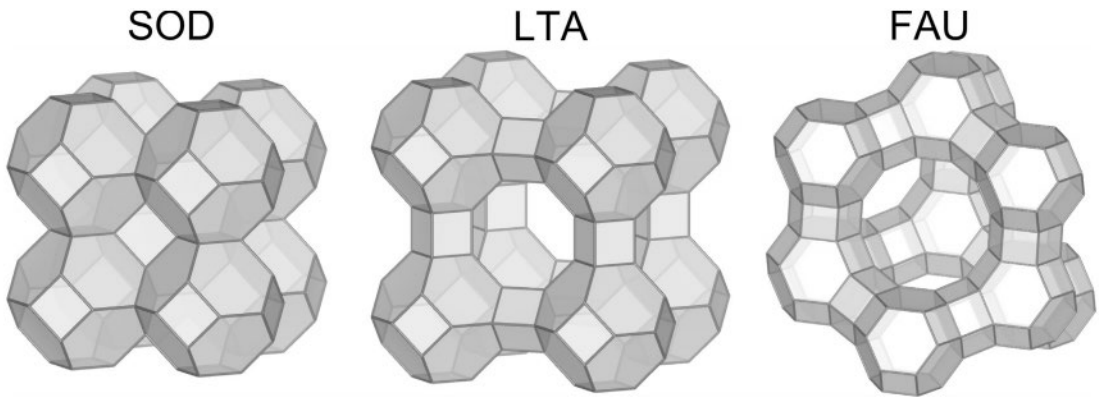

Figure 6. Illustration of the most common zeolites obtained by autoclave. Source: Rożek et al. [54].

3 ALKALI ACTIVATION REACTION OF OF CALCIUM-RICH PRECURSORS

After discussing the reaction of low-calcium precursors, it is valid to present the reaction mechanisms of AA materials formed from blast furnace slag, for example. It is known that in these cases, the precursor material is rich in calcium, and the products formed are different, being partly similar to the hydration products of Portland cement. As highlighted in the introduction, the calcium-rich precursor is defined as one with a Ca/(Si+Al) ratio higher than 1 [1]. The first distinguishing feature, which deserves to be highlighted, of the systems formed by calcium-rich precursors concerning the geopolymers previously defined is that blast furnace slag, for example, is much more reactive at moderately alkaline pH than geopolymer materials [2]. This allows the use of several other materials as an activating solution, besides sodium and potassium hydroxides and silicates, such as alkali metal carbonate or sulfate solutions. That is because BFS reacts very slowly with water and the presence of alkaline compounds only accelerates the material's hardening reaction [53].

The alkali-activated reaction products of blast furnace slag in alkali metal silicate and hydroxide solutions are generally predominantly hydrated calcium silicate gels, similar to those obtained in the hydration of Portland cement [8], [66]. However, there is an important difference, because the gels have lower amounts of Ca and more amounts of Al in tetrahedral locations. That leads to a higher degree of polymerization and also to a significant degree of crosslinking between formed gel chains. While C-S-H compounds are formed in cement hydration, in BFS alkali-activated reaction, C-A-S-H gels are formed, giving rise to minerals known as tobermorites [8], [57].

Figure 7 shows an illustration of the tobermorite. As with Portland cement systems, the C-A-S-H gel includes layers of silicate chains coordinated tetrahedrically with a Dreierketten structure. The region between the coverslips contains Ca^{2+} cations, alkalis, and hydration water chemically incorporated into the gel structure. Some alkaline cations also balance the net negative charge generated when Al^{3+} replaces Si^{4+} at the tetrahedral chain locations [1].

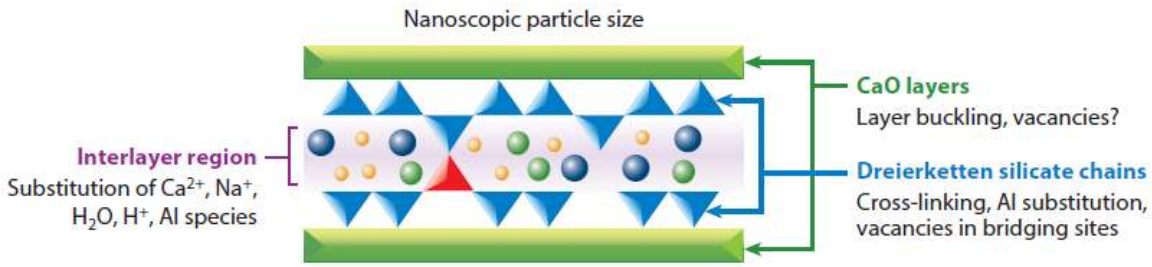

Figure 7. Tobermorite Structure. Source: Provis and Bernal [1].

However, as the amount of Al increases in the precursor's composition, Al precipitation begins to occur in the C-A-S-H chains, making it difficult for the chains to cross-link and become saturated. Thus, the precipitation of another

phase, rich in Al, occurs from the chains and impairing the formation of gels and sometimes changing the mechanical properties of the material [67].

The gels formation described is not as simple as mentioned in the previous paragraph. There is a wide formation of secondary phases that can be set up depending on the chemical composition of the studied precursors, as highlighted by Figure 8. That is because several factors, such as alkalinity, water/binder ratio, curing environment (duration, humidity, and temperature), besides the relationship among the components, the main ones being Ca, Mg, Si, Al, and Na, they affect the phases and compounds formed in the alkali-activated relationship [68], [69]. It is worth noting that the secondary phases formed are rich in Al since, as highlighted in the previous paragraph, the excess of Al causes the precipitation of other phases out of the principal C-A-S-H gels [2], [8], [57].

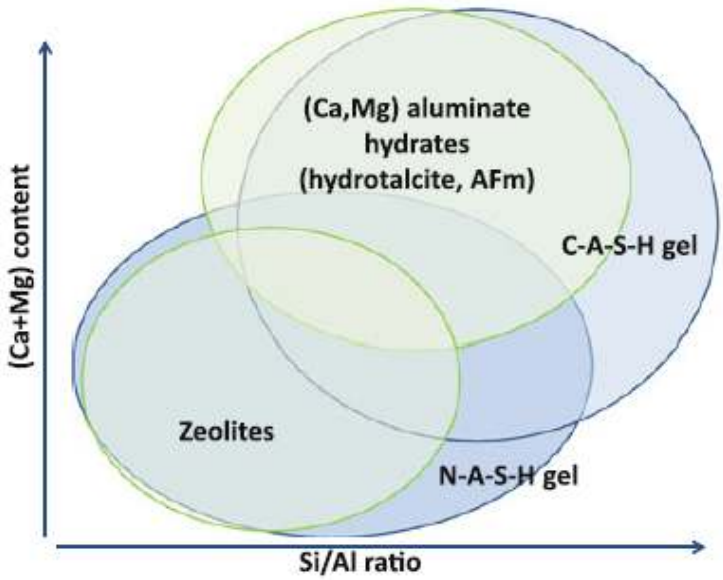

Figure 8. Formation of gels in the hydration of precursors with different calcium levels. Source: Provis [2].

Al may be substituted for Mg in C-A-S-H gels, but in very limited levels. If there is an excess of Al, and there is Mg in the material composition, another secondary compound called hydrotalcite is formed, which is often mixed with C-A-S-H gels [70]. The use of precursors with low Mg content, such as slag without this element, favors the formation of zeolites instead of hydrotalcite. Another important characteristic of secondary gels is the presence of alkali metals, such as Na, present in the activating solution. In general, alkali metals are located at the interstitial sites of the gels, producing a balance of electrical charges. However, an N-A-S-H phase can coexist as side products along with the predominant C-A-S-H phase in the alkaline activation of BFS [71]. It is known that N-A-S-H gels have a higher degree of amorphism than C-A-S-H gels and are favored in alkali activation with silicates. In the reaction with hydroxides, the formation of C-A-S-H gels is favored, presenting a high degree of crystallinity, driven by the presence of Na in the interstices of the gels [52].

The alkali activation mechanism of calcium-rich precursors is even more complex than the one of precursors low in this compound (geopolymers) and needs many studies. Besides the exemplary blast furnace slag, other materials such as steel, nickel, titanium, and phosphorous slag fit together in this group [39], [72], [73].

It is interesting to note that some researchers carried out the mixture of two different types of precursors to study the formation of alkali-activated reaction gels. The idea that reaction mechanisms occur separately for low and calcium-rich precursors is not always true in experimental research. Some studies, for example, carried out the mixture of blast furnace slag and fly ash in different proportions to study the alkaline activation of these materials together and how the gels are formed in this reaction [74], [75]. Figure 9, for example, presents a ternary diagram with the elements CaO, SiO2 and Al2O3, and the gels formed in the AA reaction. The formation of gels types C-A-S-H and N-A-S-H is verified depending on the curing age studied or depending on the material composition evaluated.

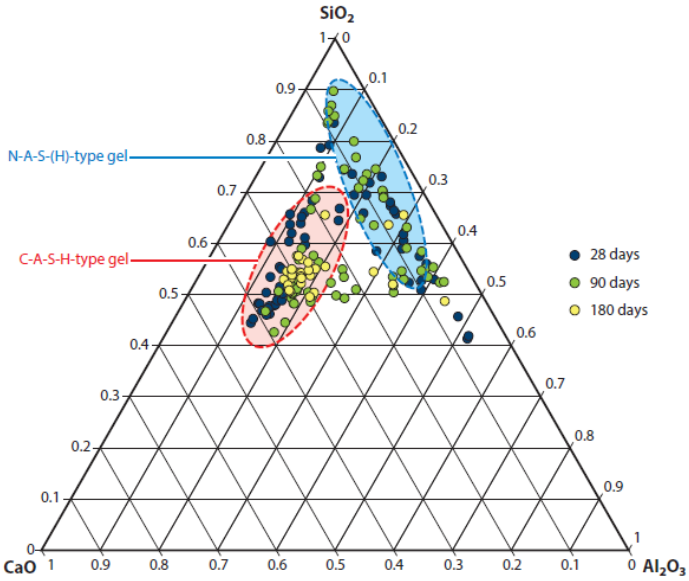

Figure 9. Ternary diagram of formation of alkaline activation gels. Source: Ismail et al. [74].

4 CHARACTERIZAION OF GELS FORMED IN THE AA REACTION

A way to identify the formation of the gels in the alkali activation reaction and to prove the mechanisms presented in the previous paragraphs is through characterization tests. Some examples of this type of assay are X-ray diffraction (XRD), transmission electron microscopy (TEM), and/or scanning electron microscopy (SEM), nuclear magnetic resonance spectrometry (NMR), and Fourier transform infrared spectroscopy (FTIR).

For the determination of the crystalline structure, one of the main techniques employed is X-ray diffraction, and it is even possible to perform the quantitative determination of zeolite since a reliable database is available [76]. This technique is very widespread in the control of zeolites industrial production [77], for example, and some authors have sought to apply it to the study of alkali-activated materials [78], [79].

The creation of the database for quantitative analysis of the zeolite phases present in the alkali-activated materials is complex, and it is necessary to use information known from the international bibliography. For example, it is possible to associate the formation of zeolite X with peaks in the 2θ values of 32º, 43.5º and 50.5º, obtained through the file of the International Center for Diffraction Data (ICDD) # 39-0218 [80]. Zeolite A, in turn, can be related to peaks in the 2θ values of 7.5º, 10.5º, 30º and 34.9º by ICDD file # 35–1009 [81], while zeolite K is detected at the peak with 2θ value of 10º by ICDD file # 22–0793 [82]. It is observed that the use of XRD for quantitative analysis of the crystalline phases formed by the alkali-activated mechanisms is not so simple, which is why several authors use a qualitative characterization, relating the appearance of the zeolitic phase peaks with the efficiency of the AA reaction.

More satisfactory results are obtained using XRD techniques in conjunction with others, such as FTIR [83], [84], or even thermogravimetric analysis (TGA) techniques [85]. In the case of the use of FTIR, it is possible to identify materials with a short-range structural order through the relation of the spectrometry obtained with standards known in the bibliography [86], [87]. That technique allows the analysis of amorphous and semi-crystalline bands within the material structure, complementing the XRD technique.

Figure 10, for example, shows the results of FTIR obtained in the geopolymers analysis based on metakaolin with partial replacement by palm oil in 5, 10, and 15% [86]. The authors found that the best resistance results were obtained with geopolymers containing 5% palm oil, attributed to the efficiency in geopolymerization. That fact was checked by the authors using FTIR, as illustrated by Figure 10, whose presence of bands in 1659, 1408, 1000, 723, 589, and 446 cm^{-1} is verified. The bands of 1659 and 1408 cm^{-1} were attributed by the authors to the presence of NaOH and free water due to the activating solution, while the bands between 800 and 400 cm^{-1} are related to the Si-O-Si bond. The most noticeable band in the figure is found at 1000 cm^{-1}, related to the stretching of the Si-O-Al bond in the reaction products. The bands observed by the authors are compatible with other published works [18], [79], [80], [84]. The authors attributed the higher resistance obtained by geopolymers with 5% palm oil to the most noticeable bands observed by this composition, which proves the efficiency of the alkaline activation reaction [86].

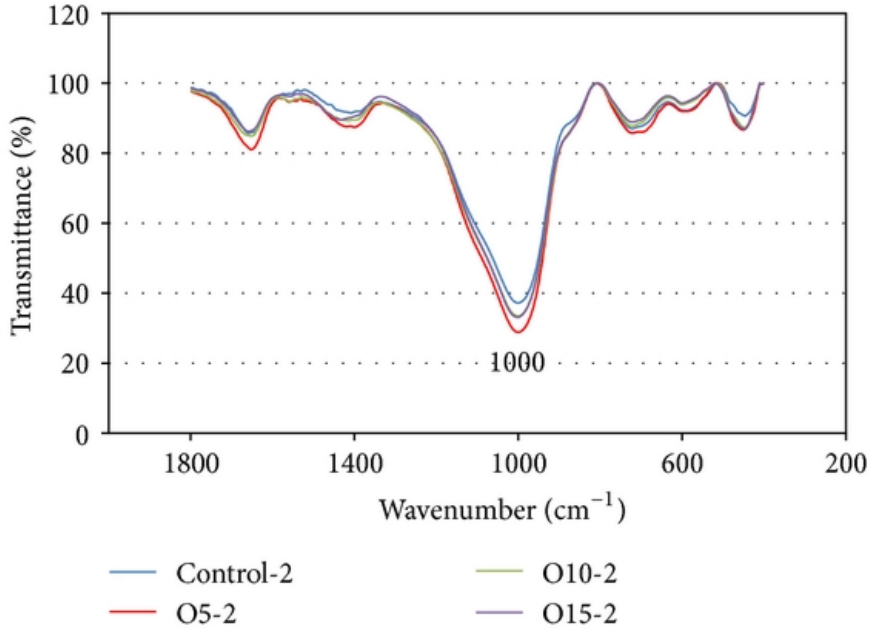

Figure 10. FTIR analysis for metakaolin geopolymers with partial incorporation of palm oil. Source: Hawa et al. [86].

Another way of characterizing the products of the AA reaction is by nuclear magnetic resonance (NMR) spectrometry, which in the case of the geopolymers study, for example, the resonance of two types of isotopes is carried out: Al^{27} e Si^{29} [39], [88], [89].

In the isotope Al^{27} resonance, analyzes are performed based on the frequency of 55 ppm, related to aluminum hydroxide, and the frequency of 76 ppm, related to sodium aluminate (Al^4), where aluminum presents coordination 4, that is, it presents 4 covalent bonds [39], [84]. The analysis of the formation of geopolymeric networks is carried out by verifying the number of covalent bonds made by Al^{27}. For example, in the case of Al^4Q^0, aluminum has 4 covalent bonds, but none of them are made with silicon, that is, it is still sodium aluminate whose frequency is 76 ppm. In the case of do Al^4Q^1, aluminum has 4 covalent bonds, but one of them is with silicon, represented by a change in the resonance frequency for an interval between 71 to 75 ppm. The same pattern occurs in Al^4Q^2, change in the resonance frequency to a value between 65 to 70 ppm, and Al^4Q^3, between 60 to 65 ppm. When aluminum makes four covalent bonds with silicon, the symbol used is Al^4Q^4, forming a three-dimensional network with a frequency between 52 to 58 ppm [90], [91]. In this way, it is possible to check the progress or the alkaline activation reaction efficiency.

In the isotope Si^{29} resonance, the reference is made using tetramethylsilane, whose frequency is -94 ppm [88]. The analysis is carried out in the same way as for the Al^{27} isotope, with the difference that the connections between silicon and aluminum, or between silicon and silicon can be studied [89]. Unlike aluminum, which can be tetravalent, pentavalent, or hexavalent, silicon has tetracoordination, which is why the Si^4Q^n symbology is not widely used. In general, only Q^n is used to represent the bonds of this type of isotope [18], [92], [93]. Knowing all the frequency patterns for the isotopes of Al^{27} and Si^{29}, it is possible to create a database and correlate these values with, for example, what is observed in the main zeolites. It is known that zeolite A has a value of -88.9 ppm and sodalite of -88.4 ppm, with Si^4Al^4 coordination [18], [94]. Thus, it is possible to identify the types of products obtained by the alkaline activation process using resonance techniques.

The morphological analysis of the alkali-activated reaction products can be observed by TEM or SEM, for example. Although some studies use the TEM technique [95], the vast majority of articles published in the AA materials area use SEM analysis, which will be presented in Figures 11-13. Figure 11 shows the SEM results obtained by the alkali-activated reaction of fly ash [10]. It is possible to identify N-A-S-H gels of amorphous and random nature, as well as crystalline gels, which correspond to zeolite P and analcime, two distinct types of zeolites.

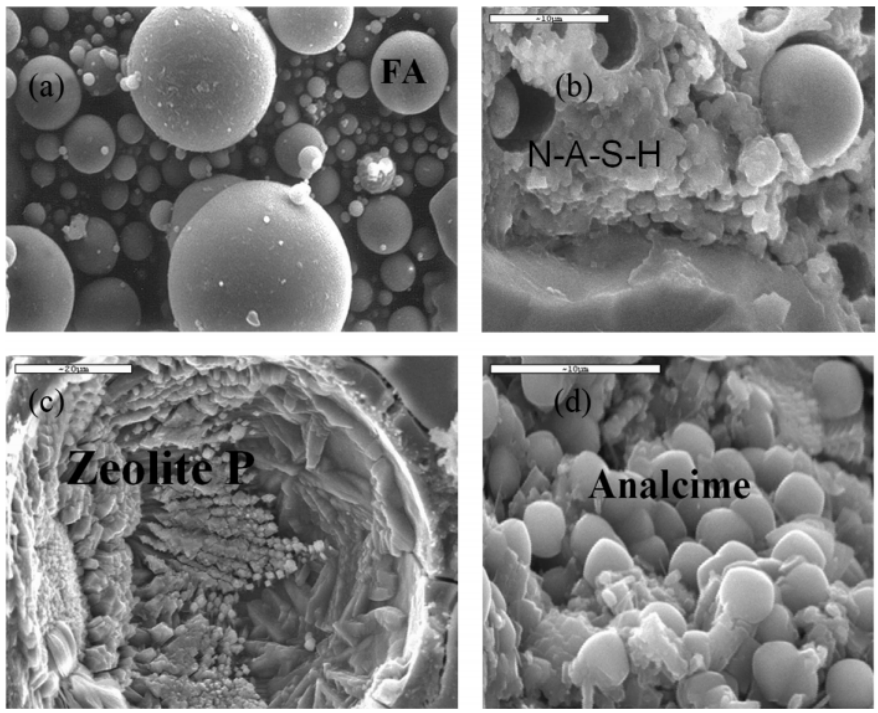

Figure 11. SEM of the activated alkali reaction of fly ash: (a) fly ash before the reaction; (b) N-A-S-H gels; (c) P zeolite gels; (d) analcime gels. Source: Palomo et al. [10].

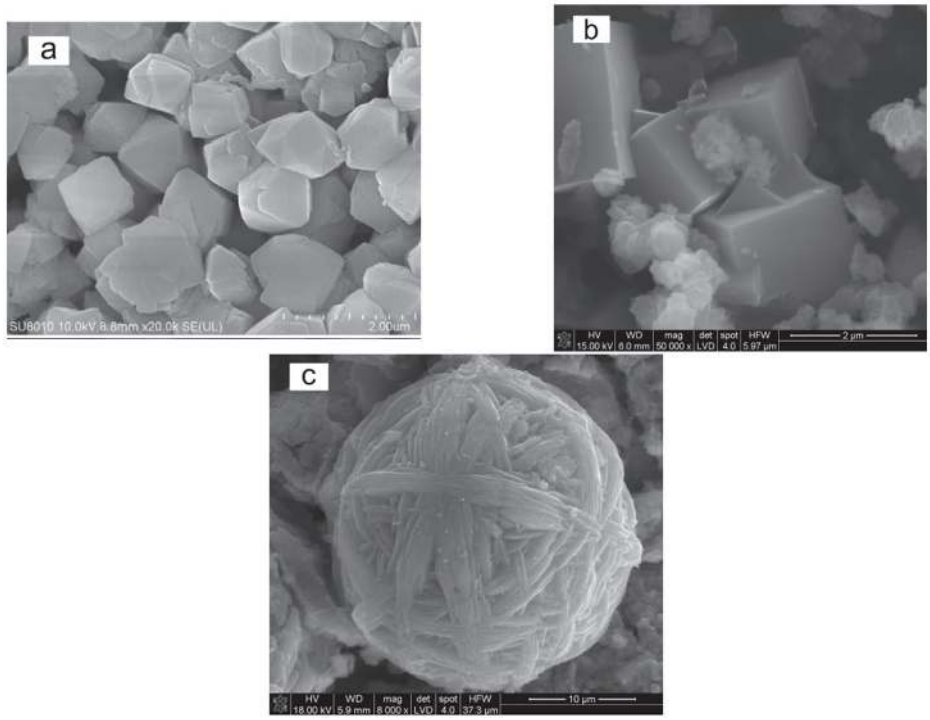

Figure 12. SEM of zeolites formed in the production of geopolymers: (a) faujasite; (b) zeolite A; (c) sodalite. Source: Rożek et al. [54].

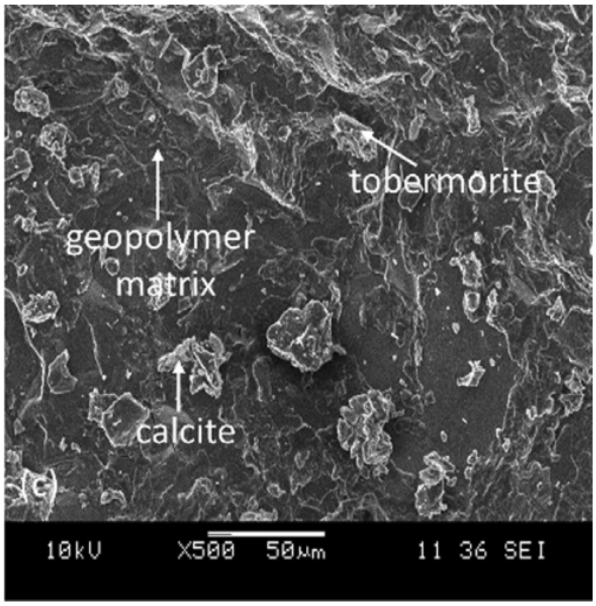

Figure 13. Morphology of tobermorite obtained in the alkaline activation of BFS. Source: Aziz et al. [99].

Figure 12 shows different zeolite gels formed in the alkali activation reaction of fly ash and metakaolin [54]. It is possible to identify faujasite, zeolite A, and sodalite gels, through the microstructural analysis of the products and the performance of additional characterization techniques mentioned above, such as XRD, FTIR and NMR [54]. These gels are very common in the formation of geopolymers. They are responsible for important properties in this material. Sodalite, for example, contributes to the crystalline structure stability and has hydrophilic properties, allowing cation exchange and the formation of stable and resistant products [96], [97].

It is considered the geopolymers' basic forming unit, and it is present even in other zeolite gels [97]. Faujasite and zeolite A gels have a more porous structure as their principal property due to their microscopy that is derived from the overlap of several sodalite cages [54], [98], as seen in Figure 6. The overlap of several sodalite cages groups makes it possible to obtain more complex and more crystalline zeolites, which have better mechanical properties, further reducing the density of the material obtained [96], [98].

On the morphological aspects formed in calcium-rich precursors, such as blast furnace slag, Figure 13 is analyzed, which shows the SEM of an BFS activated by sodium hydroxide, and silicate. The figure shows the presence of tobermorite gels (C-A-S-H), which do not have an aspect as visible as that of zeolites formed in geopolymers [99]. It is possible to prove the similarities of the formed material with those found in cementitious materials, where the C-S-H phase is verified. In addition, the Figure illustrates the presence of calcite particles mixed with tobermorite particles, making the difference between the two almost undetectable.

5 REACTION KINETICS OF ALKALI-ACTIVED

5.1 Influence of activators on the reaction kinetics of AA.

After explaining in detail the alkali-activated reactions mechanisms, it is interesting to present the factors that interfere with the reaction kinetics, that is, the factors that make these reactions faster or more efficient. One of the most important factors is related to the types of activators used in the process, as well as their viscosity and pH. Other factors are the influence of the cure type and the precursor granulometry, which modifies the reactivity of this material.

Regarding the activators, these materials are defined as hydroxides, silicates, sulfates, or carbonates of alkali metals, which, when diluted in water in a determined proportion can make the precursor harden [6]. Initially, it is necessary to highlight that the types of activators most used in research are hydroxides and silicates and that the two cause different kinetics in the AA reaction. Besides, it is usually common to use only sodium or potassium hydroxide, or even a combined solution of sodium hydroxide and silicate [13].

When using only hydroxides, there is no increase in the amount of silica in the system, while when using silicates the amount of silica in the system reaches higher levels [58]. It is known that in the AA reaction, the precursor's alumina is more reactive than silica, it is released first and available for the geopolymerization reaction in a shorter time than the silica present in the precursor [52]. Thus, the use of silicate-based activators promotes an acceleration in the reaction of geopolymerization or alkaline activation, due to the fact that the silica present in the silicate reacts more quickly with the alumina released by the precursors. The use of silicate favors the AA reaction process, leading to more resistant products than with the use of hydroxide alone [100].

It is necessary to highlight that the precursors' properties are unique and individual within each research due to issues related to granulometry and oxide composition. That makes it impossible to define an optimal amount of silica. Even so, some researchers report that the use of mixed actives containing hydroxide and sodium silicate allowed to obtain a resistance of 60 MPa at 7 days. The same authors had obtained resistance of 30 MPa at 28 days using only sodium hydroxide in alkaline activation [101]. In this research, a more resistant product was obtained in a much shorter curing time using a mixed solution composed of sodium hydroxide and silicate. The same pattern was found in other studies [30], [50], [102]. That indicates the benefits of applying silicate on the mechanical properties of alkali-activated materials.

Also, other negative factors can be cited by using only hydroxide in the solutions. When used alone, these materials are used in high molar concentrations to increase the precursor reactivity. It is noteworthy that each precursor presents exclusive parameters of reactivity, making it difficult to compare different studies. However, some authors highlight and prove this fact with experimental results [21], [51].

That high concentration can lead to significant occupational health and safety considerations in a large production facility, as these solutions are classified as corrosive under the workplace legislation in force in almost all countries in the world [1]. Also, the need for thermal curing is common when only hydroxides are used, as occurs when fly ash is used as a precursor, at temperatures of about 60ºC [55], [103]. This fact is acceptable for pre-molded parts, but it makes the molded parts on site unfeasible.

Hydroxide-activated binders, whether based on fly ash or BFS, also tend to show higher permeability than their silicate-activated equivalents and tendency to efflorescence [104]. That is because the reaction extent reached by the binder before curing is generally low, which leads to an open microstructure and higher material porosity [105]. Efflorescence and other visible effects of alkali mobility are undesirable. However, they can be overcome to some extent by appropriate control of curing conditions or by the addition of secondary aluminum sources. That ensures that a sufficient extent of reaction is achieved before the material is put into service [106], [107].

One of the disadvantages of using mixed solutions is the silicate cost, which is higher than that of hydroxides, making the alkali-activated materials production more expensive, especially when compared to Portland cement-based materials [2]. Also, the use of silicate solutions in alkaline activation impairs the viscosity of the activating solution, making it difficult to work with the paste, mortar or alkali-activated concrete used [108]. Thus, although it presents a potential to increase the mechanical resistance, problems during the structures molding due to the low workability can cause defects or pathologies in the parts and reduce its resistance and durability parameters. Another important factor in the reactions kinetics is the of the solution's molarity, in the case of the hydroxide type activator using, or of the silica modulus (Ms or s) in the case of the use together of silicates and hydroxides. These parameters are defined by Equations 2 and 3, respectively, and have simple definitions. The molarity represents the amount of of alkali metal hydroxide moles contained in a volume of solvent, usually water. The silica modulus represents the molar relationship between SiO_2 and M_2O of a system formed by silicates and hydroxides, where M represents an alkali metal, such as sodium or potassium [1], [2], [57].

$$M = \frac{[NaOH]}{V} \tag{2}$$

where M= molarity (in moles/l); [NaOH]= number of moles of sodium, calculated by dividing the mass used in the solution by the molar mass worth 40g /mol, in moles; V= volume of the solution, in l.

$$M_s = \frac{[SiO_2]}{[Na_2O]} \tag{3}$$

where Ms= silica module, dimensionless; [SiO_2]= number of moles of silicon oxide, calculated by dividing the mass used in the solution by the molar mass that is worth 60g / mol, in moles; [Na_2O]= number of moles of sodium oxide, calculated by dividing the mass used in the solution by the molar mass worth 62g / mol, in moles.

On molarity, Figure 14 presents a graph that illustrates the rate of alkali-activated reaction as a function of different molarity values obtained by the calorimetry technique (5M, 10M, 12M, 15M, and 18M). It appears that, for the precursor used by the authors, the higher the molarity, the longer the reaction takes to reach its peak. The 10 M molarity has practically the same reactivity as 12 M, while the same thing happens for 15 M and 18 M. This study's authors concluded that the use of molarity of 5M is inefficient in the alkali-activated reaction and that the most recommended values of molarity are between 10 to 18M [109].

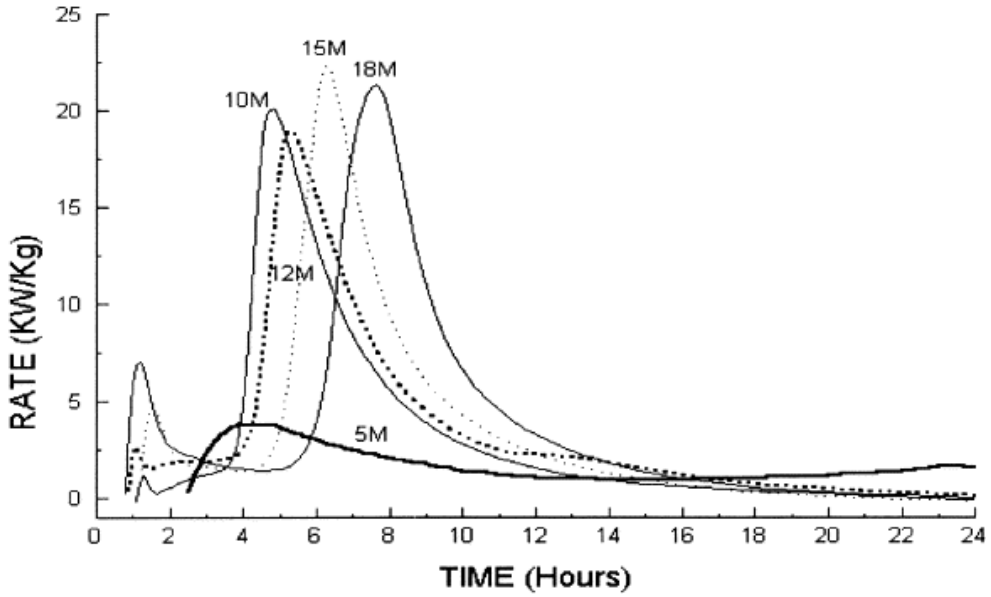

Figure 14. Calorimetry test as a function of molarity. Source: Alonso and Palomo [109].

On the silica modulus, Figure 15 shows the rates of alkali-activated reaction as a function of different values of Ms obtained by the calorimetry technique (0.6, 0.9, and 1.2) using blast furnace slag as a precursor. It appears that the higher the silica module, the higher the rate of energy released, and the higher the reactions kinetics, proving that the increase in the silica modulus accelerates and increases the reaction rates [110].

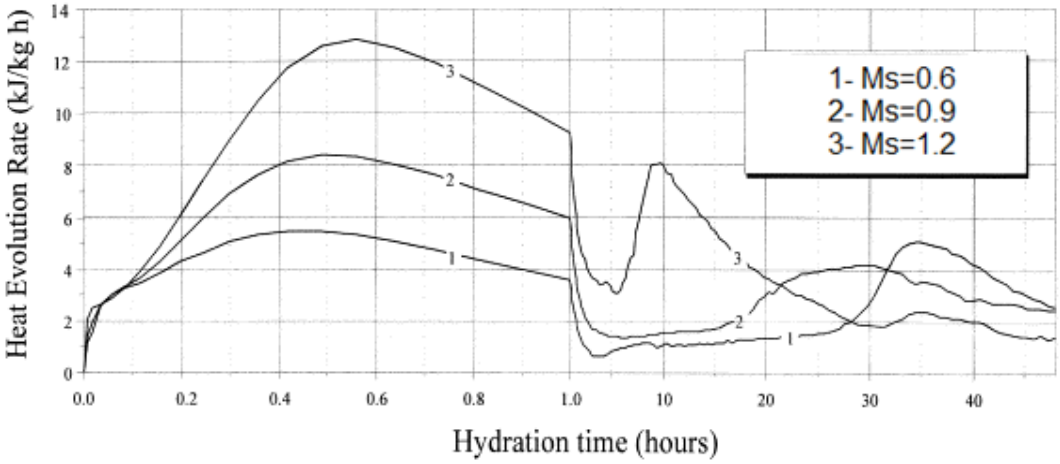

Figure 15. Calorimetry test as a function of Ms. Source: Krizan and Zivanovic [110].

There are few studies using sodium sulphate or sodium carbonate as alkaline activators, primarily because these compounds have low efficiency when compared to the hydroxides and silicates mentioned above, due to the influence of pH [111], [112]. Most research uses sulfates and carbonates together with sodium or potassium hydroxide, for example [113], in an attempt to correct the pH to values close to 14. Besides, there is a problem with using sulfate or carbonate solutions in reinforced structures because these materials can cause attack or degradation of armor [114] and can cause pathologies.

Regarding the types of alkali metals used in research, those with the highest applications are sodium and potassium. Comparing the efficiency of these two types of metals, it appears that the size of the cation is directly linked to the kinetics of the geopolymerization reactions. As Na^+ is smaller than K^+, a smaller amount of silicate oligomers is formed [115]. Therefore, it is observed that the larger the cation, the higher the reaction kinetics of the AA because the more favored is the formation of larger silicate oligomers in which $Al(OH)^{-4}$ prefers to bind. Thus, precursors activated with KOH have higher compressive strength compared to geopolymers synthesized from NaOH solutions [116]. Also, since K^+ is more basic, higher silicate dissolution rates are possible, allowing for denser and more efficient polycondensation reactions, which increase the final mechanical strength of the matrix [115].

Although there is research with other alkali metals, such as lithium and cesium, the availability of these materials is much less than that of sodium and potassium and makes research related to these materials much less frequent [117], [118]. In any case, the cation size scale is as follows: Cs> K> Na> Li. That is why it is believed that that is also the efficiency scale of the reactions kinetics of alkaline activation, that is, that cesium is the most reactive and lithium the least, comparing these four alkali metals. The results found in the bibliography confirm this pattern of reaction kinetics [118], [119].

5.2 Cure type Influence

Another very important factor in the reactions kinetics of AA is the type of cure performed in the research. Even though each precursor has its peculiarities, due to the difference in chemical composition, reactivity, and particle size, there are reports of researchers studying the alkaline activation of fly ash, metakaolin, and blast furnace slag at room temperatures (25 to 30ºC) and in a greenhouse environment (60 to 90ºC). It was found that curing performed at a temperature of 60ºC considerably increases the compressive strength of the materials [28], [120], [121]. This increase in the cure temperature favors resistance because it increases the dissolution of reactive species, such as silica and alumina, increasing the reactions kinetics [122]. However, oven curing deserves special attention since prolonged curing times distort the reactions, causing partial water evaporation with the formation of microcavities that lead to cracking of the samples, weakening the structure of the formed gels, suggesting that small amounts of structural water they need to be maintained in order to reduce cracks and maintain the integrity of the material [123], [124].

Curing at very high temperatures, above 100ºC, also impairs the alkaline activation reaction because when curing occurs at very high temperatures, the samples do not have sufficient moisture [124]. The loss of water in an accelerated and precocious way accelerates carbonation, lowers pH levels, and results in a delay in the precursors activation, resulting in a high aluminum content in the formed gels. Under these conditions, the final product is granular, porous, and characterized by low mechanical resistance [125], [126]. It appears that the most appropriate is to perform thermal curing in milder temperatures and use a not too long curing period. To illustrate this information, Table 3 presents data from several studies with different precursors cured at different temperatures, also showing the compression strength obtained.

Table 3. Interference of the curing temperature in the kinetics of the AA reaction.

Precursor Type	Temperature (ºC)	Time (days)	Compressive strength (MPa)
Fly ash	60	7	5.12
Source [120].	80	7	7.54
	120	7	7.90
	60	28	12.53
	80	28	15.21
	120	28	11.63
Blast furnace slag	60	7	35.11
Source [120].	80	7	30.78

Table 3. Continue...

Precursor Type	Temperature (ºC)	Time (days)	Compressive strength (MPa)
	120	7	40.20
	60	28	35.44
	80	28	35.80
	120	28	36.19
Fly ash	30	7	21.20
Source [123].	90	7	40.53
	30	28	24.98
	90	28	42.84
Blast furnace slag	25	7	25.16
Source [121].	60	7	40.99
	95	7	29.98
	25	28	43.52
	60	28	45.23
	95	28	31.06
Metakaolin	25	7	34.78
Source [28].	50	7	59.28
	80	7	55.72
	25	28	50.41
	50	28	60.14
	80	28	58.42
Metakaolin	30	7	7.03
Source [122].	60	7	17.87
	90	7	13.13

6 FINAL CONSIDERATIONS

This study aims to present an extensive and detailed review on the reaction mechanisms of alkali-activated materials, dividing them into two large groups, depending on the amount of calcium oxide contained in its chemical composition. Materials with reduced amounts of calcium (Ca / (Si + Al) <1) are defined as precursors of low calcium content, also named as geopolymers, and are therefore predominantly aluminum silicates. Upon undergoing geopolymeric reaction it forms compounds similar to zeolites, which are highly crystalline or nanocrystalline, but also have amorphous gels named N-A-S-H, both of which are based on polysialates. The main characteristics of these gels were discussed in the text, being approached the most studied types of precursors that fit in this class of materials, such as fly ash and metakaolin. The steps of the typical alkaline activation reaction of these materials were established, through the phases of dissolution, condensation, reorganization, polycondensation, with or without crystallization, and finally hardening.

Materials with significant amounts of calcium (Ca/(Si+Al)>1) present an alkali-activated reaction similar to Portland cement, however forming gels called C-A-S-H (tobermorite). Also, some secondary products are formed in this reaction, as is the case with N-A-S-H and hydrotalcite. The main example of a precursor that follows this reaction pattern is blast furnace slag. The characteristics of mixed gels and techniques for identifying formed gels were addressed, using X-ray diffraction (XRD), nuclear magnetic resonance spectrometry (NMR), Fourier transform infrared spectroscopy (FTIR), and scanning electronic microstructure (SEM).

Finally, a study of the reaction kinetics of alkali-activated was carried out and it was found that the type of activator solution used, such as the hydroxide-only base or the silicate and hydroxide base, modify the efficiency and speed of these reactions. Other factors, such as the type of alkali metal used (sodium, potassium), the molarity, or the silicon modulus of the solution, also affect the kinetics of the reactions. Curing factors, such as age and temperature conditions, can act as catalysts for alkali-activated reactions, and cures performed during excessive exposure times and at elevated temperatures (above 100ºC) in general impair the mechanical properties obtained from alkali-activated materials.

As suggestions for future work to improve the understanding of the reaction mechanisms of alkali-activated materials, the development of standards and procedures with exclusive application to this class of materials stands out since currently technical standards of other construction components are adopted. Other important contributions are the

development of activators with less impact than conventional silicates and hydroxides and the understanding of how these activators modify the steps and kinetics of the alkaline activation reaction.

On precursors, additional studies are needed on the interference of other oxides in the mechanisms of alkali-activated reaction. It is known that some types of industrial waste contain iron oxide, magnesium, nickel, chromium, among others. The technology of alkali-activated materials is a great contribution to the evaluation of the interferences that these compounds cause in the formation of gels and the kinetics of the alkali-activated reaction, although there is already recent research that deals with this subject in an appropriate way. However, there are still relevant issues that need further understanding and discussion regarding the influence of these metal oxides on the alkali-activated reaction. It also stands out as a suggestion the need for the development of tools that can accurately measure the degree of activation of alkali-activated binders, as well as the rheological parameters of the material, enabling the development of even more efficient materials.

Another relevant contribution is the evaluation of the production of alkali-activated materials in large scale and real size, not only through simulations in laboratories with specimens, but using beams in reduced size, for example. This type of study allows the assessment of logistics and the understanding of how the reaction mechanisms of alkali-activated materials in a proportion closer to the real one is.

ACKNOWLEDGEMENTS

The authors would like to thank FAPERJ and CNPq for their support.

REFERENCES

[1] J. L. Provis and S. A. Bernal, "Geopolymers and related alkali-activated materials," *Annu. Rev. Mater. Res.*, vol. 44, no. 1, pp. 299–327, 2014, http://dx.doi.org/10.1146/annurev-matsci-070813-113515.

[2] J. L. Provis, "Geopolymers and other alkali activated materials: why, how, and what," *Mater. Struct. Constr.*, vol. 47, no. 1-2, pp. 11–25, 2014, http://dx.doi.org/10.1617/s11527-013-0211-5.

[3] K. Komnitsas and D. Zaharaki, "Geopolymerisation: a review and prospects for the minerals industry," *Miner. Eng.*, vol. 20, no. 14, pp. 1261–1277, 2007, http://dx.doi.org/10.1016/j.mineng.2007.07.011.

[4] C. G. S. Severo, "Caracteristicas, particularidades e principios científicos dos materiais ativados alcalinamente, Rev," *Eletronica Mater. Process*, vol. 8, pp. 55–67, 2013.

[5] B. Majidi, "Geopolymer technology, from fundamentals to advanced applications: A review," *Mater. Technol.*, vol. 24, no. 2, pp. 79–87, 2009, http://dx.doi.org/10.1179/175355509X449355.

[6] F. Pacheco-Torgal, J. Castro-Gomes, and S. Jalali, "Alkali-activated binders: a review. Part 1. Historical background, terminology, reaction mechanisms and hydration products," *Constr. Build. Mater.*, vol. 22, no. 7, pp. 1305–1314, 2008, http://dx.doi.org/10.1016/j.conbuildmat.2007.10.015.

[7] J. Davidovits, “Properties of geopolymer cements,” in *1st Int. Conf. Alkaline Cem. Concr.*, 1994, pp. 131–149.

[8] J. L. Provis and J. S. J. Van Deventer, "Geopolymerisation kinetics. 1. In situ energy-dispersive X-ray diffractometry," *Chem. Eng. Sci.*, vol. 62, no. 9, pp. 2309–2317, 2007, http://dx.doi.org/10.1016/j.ces.2007.01.027.

[9] G. Habert, J. B. d’Espinose de Lacaillerie, and N. Roussel, "An environmental evaluation of geopolymer based concrete production: reviewing current research trends," *J. Clean. Prod.*, vol. 19, no. 11, pp. 1229–1238, 2011, http://dx.doi.org/10.1016/j.jclepro.2011.03.012.

[10] A. Palomo, P. Krivenko, I. Garcia-Lodeiro, E. Kavalerova, O. Maltseva, and A. Fernández-Jiménez, "A review on alkaline activation: new analytical perspectives," *Mater. Constr.*, vol. 64, no. 315, e022, 2014, http://dx.doi.org/10.3989/mc.2014.00314.

[11] J. Davidovits, L. Huaman, and R. Davidovits, "Ancient organo-mineral geopolymer in South-American Monuments: Organic matter in andesite stone. SEM and petrographic evidence," *Ceram. Int.*, vol. 45, no. 6, pp. 7385–7389, 2019, http://dx.doi.org/10.1016/j.ceramint.2019.01.024.

[12] J. Davidovits, L. Huaman, and R. Davidovits, "Ancient geopolymer in south-American monument: SEM and petrographic evidence," *Mater. Lett.*, vol. 235, pp. 120–124, 2019, http://dx.doi.org/10.1016/j.matlet.2018.10.033.

[13] F. Pacheco-Torgal, J. Castro-Gomes, and S. Jalali, "Alkali-activated binders: a review. Part 2. About materials and binders manufacture," *Constr. Build. Mater.*, vol. 22, no. 7, pp. 1315–1322, 2008, http://dx.doi.org/10.1016/j.conbuildmat.2007.03.019.

[14] M. Lahoti, K. H. Tan, and E. H. Yang, "A critical review of geopolymer properties for structural fire-resistance applications," *Constr. Build. Mater.*, vol. 221, pp. 514–526, 2019, http://dx.doi.org/10.1016/j.conbuildmat.2019.06.076.

[15] Y. Wu et al., "Geopolymer, green alkali activated cementitious material: Synthesis, applications and challenges," *Constr. Build. Mater.*, vol. 224, pp. 930–949, 2019, http://dx.doi.org/10.1016/j.conbuildmat.2019.07.112.

[16] A. R. G. Azevedo, M. T. Marvila, H. A. Rocha, L. R. Cruz, and C. M. F. Vieira, "Use of glass polishing waste in the development of ecological ceramic roof tiles by the geopolymerization process," *Int. J. Appl. Ceram. Technol.*, vol. 17, no. 6, pp. 2649–2658, 2020., http://dx.doi.org/10.1111/ijac.13585.

[17] N. R. Rakhimova and R. Z. Rakhimov, "Reaction products, structure and properties of alkali-activated metakaolin cements incorporated with supplementary materials – a review," *J. Mater. Res. Technol.*, vol. 8, no. 1, pp. 1522–1531, 2019, http://dx.doi.org/10.1016/j.jmrt.2018.07.006.

[18] R. K. Preethi and B. V. Venkatarama Reddy, "Experimental investigations on geopolymer stabilised compressed earth products," *Constr. Build. Mater.*, vol. 257, 119563, 2020, http://dx.doi.org/10.1016/j.conbuildmat.2020.119563.

[19] Z. Zhang, H. Wang, J. L. Provis, F. Bullen, A. Reid, and Y. Zhu, "Quantitative kinetic and structural analysis of geopolymers. Part 1. The activation of metakaolin with sodium hydroxide," *Thermochim. Acta*, vol. 539, pp. 23–33, 2012, http://dx.doi.org/10.1016/j.tca.2012.03.021.

[20] C. E. White, J. L. Provis, T. Proffen, D. P. Riley, and J. S. J. Van Deventer, "Density functional modeling of the local structure of kaolinite subjected to thermal dehydroxylation," *J. Phys. Chem. A*, vol. 114, no. 14, pp. 4988–4996, 2010, http://dx.doi.org/10.1021/jp911108d.

[21] T. Kovářík et al., "Thermomechanical properties of particle-reinforced geopolymer composite with various aggregate gradation of fine ceramic filler," *Constr. Build. Mater.*, vol. 143, pp. 599–606, 2017, http://dx.doi.org/10.1016/j.conbuildmat.2017.03.134.

[22] E. Kamseu, V. Catania, C. Djangang, V. M. Sglavo, and C. Leonelli, "Correlation between microstructural evolution and mechanical properties of a-quartz and alumina reinforced K-geopolymers during high temperature treatments," *Adv. Appl. Ceramics*, vol. 111, no. 3, pp. 120–128, 2012, http://dx.doi.org/10.1179/1743676111Y.0000000013.

[23] A. Elimbi, H. K. Tchakoute, and D. Njopwouo, "Effects of calcination temperature of kaolinite clays on the properties of geopolymer cements," *Constr. Build. Mater.*, vol. 25, no. 6, pp. 2805–2812, 2011, http://dx.doi.org/10.1016/j.conbuildmat.2010.12.055.

[24] A. Fernández-Jiménez, M. Monzó, M. Vicent, A. Barba, and A. Palomo, "Alkaline activation of metakaolin–fly ash mixtures: obtain of zeoceramics and zeocements," *Microporous Mesoporous Mater.*, vol. 108, no. 1-3, pp. 41–49, 2008, http://dx.doi.org/10.1016/j.micromeso.2007.03.024.

[25] R. San Nicolas, S. A. Bernal, R. Mejía De Gutiérrez, J. S. J. Van Deventer, and J. L. Provis, "Distinctive microstructural features of aged sodium silicate-activated slag concretes," *Cement Concr. Res.*, vol. 65, pp. 41–51, 2014, http://dx.doi.org/10.1016/j.cemconres.2014.07.008.

[26] J. S. J. Sindhunata, J. S. J. Van Deventer, G. C. Lukey, and H. Xu, "effect of curing temperature and silicate concentration on fly-ash-based geopolymerization," *Ind. Eng. Chem. Res.*, vol. 45, no. 10, pp. 3559–3568, 2006, http://dx.doi.org/10.1021/ie051251p.

[27] C. Kuenzel, L. J. Vandeperre, S. Donatello, A. R. Boccaccini, and C. Cheeseman, "Ambient temperature drying shrinkage and cracking in metakaolin-based geopolymers," *J. Am. Ceram. Soc.*, vol. 95, no. 10, pp. 3270–3277, 2012, http://dx.doi.org/10.1111/j.1551-2916.2012.05380.x.

[28] J. Cai, X. Li, J. Tan, and B. Vandevyvere, "Thermal and compressive behaviors of fly ash and metakaolin-based geopolymer," *J. Build. Eng.*, vol. 30, 101307, 2020, http://dx.doi.org/10.1016/j.jobe.2020.101307.

[29] Z. Sun, A. Vollpracht, and H. A. Van der Sloot, "pH dependent leaching characterization of major and trace elements from fly ash and metakaolin geopolymers," *Cement Concr. Res.*, vol. 125, 105889, 2019, http://dx.doi.org/10.1016/j.cemconres.2019.105889.

[30] J. Cai, J. Pan, X. Li, J. Tan, and J. Li, "Electrical resistivity of fly ash and metakaolin based geopolymers," *Constr. Build. Mater.*, vol. 234, 117868, 2020, http://dx.doi.org/10.1016/j.conbuildmat.2019.117868.

[31] M. Ahmaruzzaman, "A review on the utilization of fly ash," *Pror. Energy Combust. Sci.*, vol. 36, no. 3, pp. 327–363, 2010, http://dx.doi.org/10.1016/j.pecs.2009.11.003.

[32] X. F. Wu and G. Q. Chen, "Coal use embodied in globalized world economy: from source to sink through supply chain," *Renew. Sustain. Energy Rev.*, vol. 81, pp. 978–993, 2018, http://dx.doi.org/10.1016/j.rser.2017.08.018.

[33] İ. İ. Atabey, O. Karahan, C. Bilim, and C. D. Atiş, "The influence of activator type and quantity on the transport properties of class F fly ash geopolymer," *Constr. Build. Mater.*, vol. 264, 120268, 2020, http://dx.doi.org/10.1016/j.conbuildmat.2020.120268.

[34] A. M. Rashad, "A brief on high-volume Class F fly ash as cement replacement: a guide for Civil Engineer," *Int. J. Sustain. Built Environ.*, vol. 4, no. 2, pp. 278–306, 2015, http://dx.doi.org/10.1016/j.ijsbe.2015.10.002.

[35] R. Gupta, P. Bhardwaj, D. Mishra, M. Prasad, and S. S. Amritphale, "Formulation of mechanochemically evolved fly ash based hybrid inorganic-organic geopolymers with multilevel characterization," *J. Inorg. Organomet. Polym. Mater.*, vol. 27, no. 2, pp. 385–398, 2017, http://dx.doi.org/10.1007/s10904-016-0461-0.

[36] American Society for Testing and Materials, *Standard Specification for Coal Fly Ash and Raw or Calcined Natural Pozzolan for Use in Concrete*, ASTM C618-17a, 2017.

[37] F. Winnefeld, A. Leemann, M. Lucuk, P. Svoboda, and M. Neuroth, "Assessment of phase formation in alkali activated low and high calcium fly ashes in building materials," *Constr. Build. Mater.*, vol. 24, no. 6, pp. 1086–1093, 2010, http://dx.doi.org/10.1016/j.conbuildmat.2009.11.007.

[38] M. Komljenović, Z. Baščarević, and V. Bradić, "Mechanical and microstructural properties of alkali-activated fly ash geopolymers," *J. Hazard. Mater.*, vol. 181, no. 1-3, pp. 35–42, 2010, http://dx.doi.org/10.1016/j.jhazmat.2010.04.064.

[39] N. K. Lee, G. H. An, K. T. Koh, and G. S. Ryu, "Improved reactivity of fly ash-slag geopolymer by the addition of silica fume," *Adv. Mater. Sci. Eng.*, vol. 2016, pp. 1–11, 2016, http://dx.doi.org/10.1155/2016/2192053.

[40] T. Bakharev, "Geopolymeric materials prepared using Class F fly ash and elevated temperature curing," *Cement Concr. Res.*, vol. 35, no. 6, pp. 1224–1232, 2005, http://dx.doi.org/10.1016/j.cemconres.2004.06.031.

[41] N. Saboo, S. Shivhare, K. K. Kori, and A. K. Chandrappa, "Effect of fly ash and metakaolin on pervious concrete properties," *Constr. Build. Mater.*, vol. 223, pp. 322–328, 2019, http://dx.doi.org/10.1016/j.conbuildmat.2019.06.185.

[42] S. D. Khadka, P. W. Jayawickrama, S. Senadheera, and B. Segvic, "Stabilization of highly expansive soils containing sulfate using metakaolin and fly ash based geopolymer modified with lime and gypsum," *Transp. Geotechnics*, vol. 23, 100327, 2020, http://dx.doi.org/10.1016/j.trgeo.2020.100327.

[43] A. Buchwald, M. Hohmann, K. Posern, and E. Brendler, "The suitability of thermally activated illite/smectite clay as raw material for geopolymer binders," *Appl. Clay Sci.*, vol. 46, no. 3, pp. 300–304, 2009, http://dx.doi.org/10.1016/j.clay.2009.08.026.

[44] D. M. González-García, L. Téllez-Jurado, F. J. Jiménez-Álvarez, and H. Balmori-Ramírez, "Structural study of geopolymers obtained from alkali-activated natural pozzolan feldspars," *Ceram. Int.*, vol. 43, no. 2, pp. 2606–2613, 2017, http://dx.doi.org/10.1016/j.ceramint.2016.11.070.

[45] L. Tian, W. Feng, H. Ma, S. Zhang, and H. Shi, "Investigation on the microstructure and mechanism of geopolymer with different proportion of quartz and K-feldspar," *Constr. Build. Mater.*, vol. 147, pp. 543–549, 2017, http://dx.doi.org/10.1016/j.conbuildmat.2017.04.102.

[46] J. N. Yankwa Djobo, A. Elimbi, H. K. Tchakouté, and S. Kumar, "Mechanical activation of volcanic ash for geopolymer synthesis: effect on reaction kinetics, gel characteristics, physical and mechanical properties," *RSC Advances*, vol. 6, no. 45, pp. 39106–39117, 2016, http://dx.doi.org/10.1039/C6RA03667H.

[47] H. Xu and J. S. J. Van Deventer, "Factors affecting the geopolymerization of alkali-feldspars, Mining," *Metall. Explor.*, vol. 19, pp. 209–214, 2002, http://dx.doi.org/10.1007/BF03403271.

[48] Y. J. N. Djobo, A. Elimbi, J. Dika Manga, and I. B. Djon Li Ndjock, "Partial replacement of volcanic ash by bauxite and calcined oyster shell in the synthesis of volcanic ash-based geopolymers," *Constr. Build. Mater.*, vol. 113, pp. 673–681, 2016, http://dx.doi.org/10.1016/j.conbuildmat.2016.03.104.

[49] J. N. Y. Djobo, A. Elimbi, H. K. Tchakouté, and S. Kumar, "Volcanic ash-based geopolymer cements/concretes: the current state of the art and perspectives," *Environ. Sci. Pollut. Res. Int.*, vol. 24, no. 5, pp. 4433–4446, 2017, http://dx.doi.org/10.1007/s11356-016-8230-8.

[50] A. R. G. Azevedo, C. M. F. Vieira, W. M. Ferreira, K. C. P. Faria, L. G. Pedroti, and B. C. Mendes, "Potential use of ceramic waste as precursor in the geopolymerization reaction for the production of ceramic roof tiles," *J. Build. Eng.*, vol. 29, 101156, 2020, http://dx.doi.org/10.1016/j.jobe.2019.101156.

[51] L. Mo, L. Lv, M. Deng, and J. Qian, "Influence of fly ash and metakaolin on the microstructure and compressive strength of magnesium potassium phosphate cement paste," *Cement Concr. Res.*, vol. 111, pp. 116–129, 2018, http://dx.doi.org/10.1016/j.cemconres.2018.06.003.

[52] P. Duxson, S. W. Mallicoat, G. C. Lukey, W. M. Kriven, and J. S. J. Van Deventer, "The effect of alkali and Si/Al ratio on the development of mechanical properties of metakaolin-based geopolymers," *Colloids Surf. A Physicochem. Eng. Asp.*, vol. 292, no. 1, pp. 8–20, 2007, http://dx.doi.org/10.1016/j.colsurfa.2006.05.044.

[53] P. Duxson, A. Fernández-Jiménez, J. L. Provis, G. C. Lukey, A. Palomo, and J. S. J. Van Deventer, "Geopolymer technology: the current state of the art," *J. Mater. Sci.*, vol. 42, no. 9, pp. 2917–2933, 2007, http://dx.doi.org/10.1007/s10853-006-0637-z.

[54] P. Rożek, M. Król, and W. Mozgawa, "Geopolymer-zeolite composites: a review," *J. Clean. Prod.*, vol. 230, pp. 557–579, 2019, http://dx.doi.org/10.1016/j.jclepro.2019.05.152.

[55] E. Najafi Kani, A. Allahverdi, and J. L. Provis, "Calorimetric study of geopolymer binders based on natural pozzolan," *J. Therm. Anal. Calorim.*, vol. 127, no. 3, pp. 2181–2190, 2017, http://dx.doi.org/10.1007/s10973-016-5850-7.

[56] D. Van Gucht, O. Van den Bergh, T. Beckers, and D. Vansteenwegen, "Smoking behavior in context: where and when do people smoke," *J. Behav. Ther. Exp. Psychiatry*, vol. 41, no. 2, pp. 172–177, 2010, http://dx.doi.org/10.1016/j.jbtep.2009.12.004.

[57] J. L. Provis and J. S. J. Van Deventer, "Geopolymerisation kinetics. 2. Reaction kinetic modelling," *Chem. Eng. Sci.*, vol. 62, no. 9, pp. 2318–2329, 2007, http://dx.doi.org/10.1016/j.ces.2007.01.028.

[58] M. Nakai et al., "Synthesis of high silica *BEA type ferrisilicate (Fe-Beta) by dry gel conversion method using dealuminated zeolites and its catalytic performance on acetone to olefins (ATO) reaction," *Microporous Mesoporous Mater.*, vol. 273, pp. 189–195, 2019, http://dx.doi.org/10.1016/j.micromeso.2018.06.008.

[59] E. Kamseu, C. R. Kaze, J. N. N. Fekoua, U. C. Melo, S. Rossignol, and C. Leonelli, "Ferrisilicates formation during the geopolymerization of natural Fe-rich aluminosilicate precursors," *Mater. Chem. Phys.*, vol. 240, 122062, 2020, http://dx.doi.org/10.1016/j.matchemphys.2019.122062.

[60] R. C. Kaze et al., "Microstructure and engineering properties of Fe2O3(FeO)-Al2O3-SiO2 based geopolymer composites," *J. Clean. Prod.*, vol. 199, pp. 849–859, 2018, http://dx.doi.org/10.1016/j.jclepro.2018.07.171.

[61] M. Khatamian, A. A. Khandar, M. Haghighi, M. Ghadiri, and M. Darbandi, "Synthesis, characterization and acidic properties of nanopowder ZSM-5 type ferrisilicates in the Na+/K+ alkali system," *Powder Technol.*, vol. 203, no. 3, pp. 503–509, 2010, http://dx.doi.org/10.1016/j.powtec.2010.06.012.

[62] M. Król, P. Rożek, D. Chlebda, and W. Mozgawa, "Influence of alkali metal cations/type of activator on the structure of alkali-activated fly ash – ATR-FTIR studies, Spectrochim. Acta Part A Mol," *Biomol. Spectrosc.*, vol. 198, pp. 33–37, 2018, http://dx.doi.org/10.1016/j.saa.2018.02.067.

[63] A. Nikolov, H. Nugteren, and I. Rostovsky, "Optimization of geopolymers based on natural zeolite clinoptilolite by calcination and use of aluminate activators," *Constr. Build. Mater.*, vol. 243, 118257, 2020, http://dx.doi.org/10.1016/j.conbuildmat.2020.118257.

[64] P. Y. He, Y. J. Zhang, H. Chen, Z. C. Han, and L. C. Liu, "Low-cost and facile synthesis of geopolymer-zeolite composite membrane for chromium(VI) separation from aqueous solution," *J. Hazard. Mater.*, vol. 392, 122359, 2020, http://dx.doi.org/10.1016/j.jhazmat.2020.122359.

[65] C. A. Rees, J. L. Provis, G. C. Lukey, and J. S. J. Van Deventer, "Attenuated total reflectance fourier transform infrared analysis of fly ash geopolymer gel aging," *Langmuir*, vol. 23, no. 15, pp. 8170–8179, 2007, http://dx.doi.org/10.1021/la700713g.

[66] J. L. Provis, P. A. Walls, and J. S. J. Van Deventer, "Geopolymerisation kinetics. 3. Effects of Cs and Sr salts," *Chem. Eng. Sci.*, vol. 63, no. 18, pp. 4480–4489, 2008, http://dx.doi.org/10.1016/j.ces.2008.06.008.

[67] J. F. Rivera, N. Cristelo, A. Fernández-Jiménez, and R. Mejía de Gutiérrez, "Synthesis of alkaline cements based on fly ash and metallurgic slag: Optimisation of the SiO_2/Al_2O_3 and Na_2O/SiO_2 molar ratios using the response surface methodology," *Constr. Build. Mater.*, vol. 213, pp. 424–433, 2019, http://dx.doi.org/10.1016/j.conbuildmat.2019.04.097.

[68] I. Perná and T. Hanzlíček, "The setting time of a clay-slag geopolymer matrix: the influence of blast-furnace-slag addition and the mixing method," *J. Clean. Prod.*, vol. 112, pp. 1150–1155, 2016, http://dx.doi.org/10.1016/j.jclepro.2015.05.069.

[69] H. M. Khater, "Development and characterization of sustainable lightweight geopolymer composites," *Ceramica*, vol. 65, no. 373, pp. 153–161, 2019, http://dx.doi.org/10.1590/0366-69132019653732551.

[70] T. Yang, Q. Wu, H. Zhu, and Z. Zhang, "Geopolymer with improved thermal stability by incorporating high-magnesium nickel slag," *Constr. Build. Mater.*, vol. 155, pp. 475–484, 2017, http://dx.doi.org/10.1016/j.conbuildmat.2017.08.081.

[71] S. Jena and R. Panigrahi, "Performance assessment of geopolymer concrete with partial replacement of ferrochrome slag as coarse aggregate," *Constr. Build. Mater.*, vol. 220, pp. 525–537, 2019, http://dx.doi.org/10.1016/j.conbuildmat.2019.06.045.

[72] J. Qiu, Y. Zhao, J. Xing, and X. Sun, "Fly ash/blast furnace slag-based geopolymer as a potential binder for mine backfilling: effect of binder type and activator concentration," *Adv. Mater. Sci. Eng.*, vol. 2019, pp. 1–12, 2019, http://dx.doi.org/10.1155/2019/2028109.

[73] T. Bai, Z.-G. Song, Y.-G. Wu, X.-D. Hu, and H. Bai, "Influence of steel slag on the mechanical properties and curing time of metakaolin geopolymer," *Ceram. Int.*, vol. 44, no. 13, pp. 15706–15713, 2018, http://dx.doi.org/10.1016/j.ceramint.2018.05.243.

[74] I. Ismail, S. A. Bernal, J. L. Provis, R. San Nicolas, S. Hamdan, and J. S. J. Van Deventer, "Modification of phase evolution in alkali-activated blast furnace slag by the incorporation of fly ash," *Cement Concr. Compos.*, vol. 45, pp. 125–135, 2014, http://dx.doi.org/10.1016/j.cemconcomp.2013.09.006.

[75] I. Garcia-Lodeiro, A. Palomo, A. Fernández-Jiménez, and D. E. MacPhee, "Compatibility studies between N-A-S-H and C-A-S-H gels. Study in the ternary diagram Na_2O-CaO-Al_2O_3-SiO_2-H_2O," *Cement Concr. Res.*, vol. 41, no. 9, pp. 923–931, 2011, http://dx.doi.org/10.1016/j.cemconres.2011.05.006.

[76] M. Javed et al., "A facile solvent-free synthesis strategy for Co-imbedded zeolite-based Fischer-Tropsch catalysts for direct gasoline production," *Chin. J. Catal.*, vol. 41, no. 4, pp. 604–612, 2020, http://dx.doi.org/10.1016/S1872-2067(19)63436-4.

[77] S. Shahsavari and S. M. Sadrameli, "Production of renewable aromatics and heterocycles by catalytic pyrolysis of biomass resources using rhenium and tin promoted ZSM-5 zeolite catalysts," *Process Saf. Environ. Prot.*, vol. 141, pp. 305–320, 2020, http://dx.doi.org/10.1016/j.psep.2020.04.023.

[78] J. Mishra, S. Kumar Das, R. S. Krishna, B. Nanda, S. Kumar Patro, and S. Mohammed Mustakim, "Synthesis and characterization of a new class of geopolymer binder utilizing ferrochrome ash (FCA) for sustainable industrial waste management," *Mater. Today Proc.*, vol. 33, pp. 5001–5006, 2020., http://dx.doi.org/10.1016/j.matpr.2020.02.832.

[79] B. B. Jindal and R. Sharma, "The effect of nanomaterials on properties of geopolymers derived from industrial by-products: A state-of-the-art review," *Constr. Build. Mater.*, vol. 252, 119028, 2020, http://dx.doi.org/10.1016/j.conbuildmat.2020.119028.

[80] C.-L. Hwang and T.-P. Huynh, "Effect of alkali-activator and rice husk ash content on strength development of fly ash and residual rice husk ash-based geopolymers," *Constr. Build. Mater.*, vol. 101, pp. 1–9, 2015, http://dx.doi.org/10.1016/j.conbuildmat.2015.10.025.

[81] N.-E.-H. Fardjaoui, F. Z. El Berrichi, and F. Ayari, "Kaolin-issued zeolite A as efficient adsorbent for Bezanyl Yellow and Nylomine Green anionic dyes," *Microporous Mesoporous Mater.*, vol. 243, pp. 91–101, 2017, http://dx.doi.org/10.1016/j.micromeso.2017.01.008.

[82] D. Sha, B. Pan, and Y. Sun, "Investigation on mechanical properties and microstructure of coal-based synthetic natural gas slag (CSNGS) geopolymer," *Constr. Build. Mater.*, vol. 259, 119793, 2020, http://dx.doi.org/10.1016/j.conbuildmat.2020.119793.

[83] H. M. Khater, "Effect of silica fume on the characterization of the geopolymer materials," *Int. J. Adv. Struct. Eng.*, vol. 5, no. 1, pp. 12, 2013, http://dx.doi.org/10.1186/2008-6695-5-12.

[84] M. A. Pereira, D. C. L. Vasconcelos, and W. L. Vasconcelos, "Synthetic aluminosilicates for geopolymer production," *Mater. Res.*, vol. 22, no. 2, e20180508, 2019, http://dx.doi.org/10.1590/1980-5373-mr-2018-0508.

[85] T. S. Osholana, M. K. Dludlu, B. Oboirien, and R. Sadiku, "Enhanced reactivity of geopolymers produced from fluidized bed combustion bottom ash," *S. Afr. J. Chem. Eng.*, vol. 34, pp. 72–77, 2020., http://dx.doi.org/10.1016/j.sajce.2020.06.006.

[86] A. Hawa, D. Tonnayopas, and W. Prachasaree, "Performance evaluation and microstructure characterization of metakaolin-based geopolymer containing oil palm ash," *Scientific World Journal*, vol. 2013, pp. 1–9, 2013, http://dx.doi.org/10.1155/2013/857586.

[87] S. Hu et al., "Synthesis of rare earth tailing-based geopolymer for efficiently immobilizing heavy metals," *Constr. Build. Mater.*, vol. 254, 119273, 2020, http://dx.doi.org/10.1016/j.conbuildmat.2020.119273.

[88] H. Celerier et al., "Relation between working properties and structural properties from ^{27}Al, ^{29}Si and ^{31}P NMR and XRD of acid-based geopolymers from 25 to 1000°C," *Mater. Chem. Phys.*, vol. 228, pp. 293–302, 2019, http://dx.doi.org/10.1016/j.matchemphys.2019.02.049.

[89] C. Dupuy, A. Gharzouni, I. Sobrados, N. Texier-Mandoki, X. Bourbon, and S. Rossignol, "^{29}Si, ^{27}Al, ^{31}P and ^{11}B magic angle spinning nuclear magnetic resonance study of the structural evolutions induced by the use of phosphor- and boron–based additives in geopolymer mixtures," *J. Non-Cryst. Solids*, vol. 521, 119541, 2019, http://dx.doi.org/10.1016/j.jnoncrysol.2019.119541.

[90] Q. Wan, Y. Zhang, and R. Zhang, "Using mechanical activation of quartz to enhance the compressive strength of metakaolin based geopolymers," *Cement Concr. Compos.*, vol. 111, 103635, 2020, http://dx.doi.org/10.1016/j.cemconcomp.2020.103635.

[91] Q. Tian, B. Guo, and K. Sasaki, "Immobilization mechanism of Se oxyanions in geopolymer: Effects of alkaline activators and calcined hydrotalcite additive," *J. Hazard. Mater.*, vol. 387, 121994, 2020, http://dx.doi.org/10.1016/j.jhazmat.2019.121994.

[92] X. Tian, W. Xu, S. Song, F. Rao, and L. Xia, "Effects of curing temperature on the compressive strength and microstructure of copper tailing-based geopolymers," *Chemosphere*, vol. 253, 126754, 2020, http://dx.doi.org/10.1016/j.chemosphere.2020.126754.

[93] Y.-L. Tsai, J. V. Hanna, Y.-L. Lee, M. E. Smith, and J. C. C. Chan, "Solid-state NMR study of geopolymer prepared by sol–gel chemistry," *J. Solid State Chem.*, vol. 183, no. 12, pp. 3017–3022, 2010, http://dx.doi.org/10.1016/j.jssc.2010.10.008.

[94] S. Greiser, P. Sturm, G. J. G. Gluth, M. Hunger, and C. Jäger, "Differentiation of the solid-state NMR signals of gel, zeolite phases and water species in geopolymer-zeolite composites," *Ceram. Int.*, vol. 43, no. 2, pp. 2202–2208, 2017, http://dx.doi.org/10.1016/j.ceramint.2016.11.004.

[95] M. Falah and K. J. D. MacKenzie, "Synthesis and properties of novel photoactive composites of P25 titanium dioxide and copper (I) oxide with inorganic polymers," *Ceram. Int.*, vol. 41, no. 10, pp. 13702–13708, 2015, http://dx.doi.org/10.1016/j.ceramint.2015.07.198.

[96] H. Baykara, M. H. Cornejo, R. Murillo, A. Gavilanes, C. Paredes, and J. Elsen, "Preparation, characterization and reaction kinetics of green cement: ecuadorian natural mordenite-based geopolymers," *Mater. Struct.*, vol. 50, no. 3, 188, 2017, http://dx.doi.org/10.1617/s11527-017-1057-z.

[97] T. Bakharev, "Thermal behaviour of geopolymers prepared using class F fly ash and elevated temperature curing," *Cement Concr. Res.*, vol. 36, no. 6, pp. 1134–1147, 2006, http://dx.doi.org/10.1016/j.cemconres.2006.03.022.

[98] A. Buchwald, H.-D. Zellmann, and C. Kaps, "Condensation of aluminosilicate gels-model system for geopolymer binders," *J. Non-Cryst. Solids*, vol. 357, no. 5, pp. 1376–1382, 2011, http://dx.doi.org/10.1016/j.jnoncrysol.2010.12.036.

[99] I. H. Aziz, M. M. A. B. Abdullah, M. A. A. Mohd Salleh, E. A. Azimi, J. Chaiprapa, and A. V. Sandu, "Strength development of solely ground granulated blast furnace slag geopolymers," *Constr. Build. Mater.*, vol. 250, 118720, 2020, http://dx.doi.org/10.1016/j.conbuildmat.2020.118720.

[100] K. Sagoe-Crentsil and L. Weng, "Dissolution processes, hydrolysis and condensation reactions during geopolymer synthesis: part II. High Si/Al ratio systems," *J. Mater. Sci.*, vol. 42, no. 9, pp. 3007–3014, 2007, http://dx.doi.org/10.1007/s10853-006-0818-9.

[101] E. Altan and S. T. Erdoğan, "Alkali activation of a slag at ambient and elevated temperatures," *Cement Concr. Compos.*, vol. 34, no. 2, pp. 131–139, 2012, http://dx.doi.org/10.1016/j.cemconcomp.2011.08.003.

[102] M. A. Villaquirán-Caicedo and R. M. de Gutiérrez, "Synthesis of ceramic materials from ecofriendly geopolymer precursors," *Mater. Lett.*, vol. 230, pp. 300–304, 2018, http://dx.doi.org/10.1016/j.matlet.2018.07.128.

[103] A. Fernández-Jiménez, A. Palomo, and M. Criado, "Microstructure development of alkali-activated fly ash cement: a descriptive model," *Cement Concr. Res.*, vol. 35, no. 6, pp. 1204–1209, 2005, http://dx.doi.org/10.1016/j.cemconres.2004.08.021.

[104] Y. Wang et al., "Effects of Si/Al ratio on the efflorescence and properties of fly ash based geopolymer," *J. Clean. Prod.*, vol. 244, 118852, 2020, http://dx.doi.org/10.1016/j.jclepro.2019.118852.

[105] Z. Zhang, J. L. Provis, X. Ma, A. Reid, and H. Wang, "Efflorescence and subflorescence induced microstructural and mechanical evolution in fly ash-based geopolymers," *Cement Concr. Compos.*, vol. 92, pp. 165–177, 2018, http://dx.doi.org/10.1016/j.cemconcomp.2018.06.010.

[106] X. Xue, Y.-L. Liu, J.-G. Dai, C.-S. Poon, W.-D. Zhang, and P. Zhang, "Inhibiting efflorescence formation on fly ash–based geopolymer via silane surface modification," *Cement Concr. Compos.*, vol. 94, pp. 43–52, 2018, http://dx.doi.org/10.1016/j.cemconcomp.2018.08.013.

[107] M. A. Longhi, E. D. Rodríguez, B. Walkley, Z. Zhang, and A. P. Kirchheim, "Metakaolin-based geopolymers: Relation between formulation, physicochemical properties and efflorescence formation," *Compos., Part B Eng.*, vol. 182, 107671, 2020, http://dx.doi.org/10.1016/j.compositesb.2019.107671.

[108] A. J. Allen, J. J. Thomas, and H. M. Jennings, "Composition and density of nanoscale calcium-silicate-hydrate in cement," *Nat. Mater.*, vol. 6, no. 4, pp. 311–316, 2007, http://dx.doi.org/10.1038/nmat1871.

[109] S. Alonso and A. Palomo, "Calorimetric study of alkaline activation of calcium hydroxide–metakaolin solid mixtures," *Cement Concr. Res.*, vol. 31, no. 1, pp. 25–30, 2001, http://dx.doi.org/10.1016/S0008-8846(00)00435-X.

[110] D. Krizan and B. Zivanovic, "Effects of dosage and modulus of water glass on early hydration of alkali–slag cements," *Cement Concr. Res.*, vol. 32, no. 8, pp. 1181–1188, 2002, http://dx.doi.org/10.1016/S0008-8846(01)00717-7.

[111] H. Alghamdi and N. Neithalath, "Novel synthesis of lightweight geopolymer matrices from fly ash through carbonate-based activation," *Mater. Today Commun.*, vol. 17, pp. 266–277, 2018, http://dx.doi.org/10.1016/j.mtcomm.2018.09.014.

[112] J. Ahn, W.-S. Kim, and W. Um, "Development of metakaolin-based geopolymer for solidification of sulfate-rich HyBRID sludge waste," *J. Nucl. Mater.*, vol. 518, pp. 247–255, 2019, http://dx.doi.org/10.1016/j.jnucmat.2019.03.008.

[113] Q. Lv, L. Jiang, B. Ma, B. Zhao, and Z. Huo, "A study on the effect of the salt content on the solidification of sulfate saline soil solidified with an alkali-activated geopolymer," *Constr. Build. Mater.*, vol. 176, pp. 68–74, 2018, http://dx.doi.org/10.1016/j.conbuildmat.2018.05.013.

[114] A. Aboulayt, M. Riahi, M. Ouazzani Touhami, H. Hannache, M. Gomina, and R. Moussa, "Properties of metakaolin based geopolymer incorporating calcium carbonate," *Adv. Powder Technol.*, vol. 28, no. 9, pp. 2393–2401, 2017, http://dx.doi.org/10.1016/j.apt.2017.06.022.

[115] A. Hosan, S. Haque, and F. Shaikh, "Compressive behaviour of sodium and potassium activators synthetized fly ash geopolymer at elevated temperatures: a comparative study," *J. Build. Eng.*, vol. 8, pp. 123–130, 2016, http://dx.doi.org/10.1016/j.jobe.2016.10.005.

[116] T. da S. Rocha, D. P. Dias, F. C. C. França, R. R. S. Guerra, and L. R. C. O. Marques, "Metakaolin-based geopolymer mortars with different alkaline activators (Na + and K +)," *Constr. Build. Mater.*, vol. 178, pp. 453–461, 2018, http://dx.doi.org/10.1016/j.conbuildmat.2018.05.172.

[117] J. Yuan et al., "Thermal evolution of lithium ion substituted cesium-based geopolymer under high temperature treatment, Part I: Effects of holding temperature," *Ceram. Int.*, vol. 44, no. 9, pp. 10047–10054, 2018, http://dx.doi.org/10.1016/j.ceramint.2018.02.179.

[118] J. Wang, L. Han, Z. Liu, and D. Wang, "Setting controlling of lithium slag-based geopolymer by activator and sodium tetraborate as a retarder and its effects on mortar properties," *Cement Concr. Compos.*, vol. 110, 103598, 2020, http://dx.doi.org/10.1016/j.cemconcomp.2020.103598.

[119] J. L. Bell, P. E. Driemeyer, and W. M. Kriven, "Formation of ceramics from metakaolin-based geopolymers: Part I-Cs-based geopolymer," *J. Am. Ceram. Soc.*, vol. 92, no. 1, pp. 1–8, 2009, http://dx.doi.org/10.1111/j.1551-2916.2008.02790.x.

[120] G. Kastiukas, S. Ruan, S. Liang, and X. Zhou, "Development of precast geopolymer concrete via oven and microwave radiation curing with an environmental assessment," *J. Clean. Prod.*, vol. 255, 120290, 2020, http://dx.doi.org/10.1016/j.jclepro.2020.120290.

[121] M. Nasir, M. A. M. Johari, M. Maslehuddin, M. O. Yusuf, and M. A. Al-Harthi, "Influence of heat curing period and temperature on the strength of silico-manganese fume-blast furnace slag-based alkali-activated mortar," *Constr. Build. Mater.*, vol. 251, 118961, 2020, http://dx.doi.org/10.1016/j.conbuildmat.2020.118961.

[122] M. S. Muñiz-Villarreal et al., "The effect of temperature on the geopolymerization process of a metakaolin-based geopolymer," *Mater. Lett.*, vol. 65, no. 6, pp. 995–998, 2011, http://dx.doi.org/10.1016/j.matlet.2010.12.049.

[123] W. I. Wan Mastura, H. Kamarudin, I. Khairul Nizar, M. M. Al Bakri Abdullah, and H. Mohammed, "The effect of curing time on the properties of fly ash-based geopolymer bricks," *Adv. Mat. Res.*, vol. 626, pp. 937–941, 2012., http://dx.doi.org/10.4028/www.scientific.net/AMR.626.937.

[124] G. Kovalchuk, A. Fernández-Jiménez, and A. Palomo, "Alkali-activated fly ash: effect of thermal curing conditions on mechanical and microstructural development – Part II," *Fuel*, vol. 86, no. 3, pp. 315–322, 2007, http://dx.doi.org/10.1016/j.fuel.2006.07.010.

[125] M. Criado, A. Fernández-Jiménez, and A. Palomo, "Alkali activation of fly ash. Part III: effect of curing conditions on reaction and its graphical description," *Fuel*, vol. 89, no. 11, pp. 3185–3192, 2010, http://dx.doi.org/10.1016/j.fuel.2010.03.051.

[126] M. Criado, A. Fernández Jiménez, I. Sobrados, A. Palomo, and J. Sanz, "Effect of relative humidity on the reaction products of alkali activated fly ash," *J. Eur. Ceram. Soc.*, vol. 32, no. 11, pp. 2799–2807, 2012, http://dx.doi.org/10.1016/j.jeurceramsoc.2011.11.036.

Author contributions: MTM: conceptualization, writing, formal analysis, revision. ARGA, CMFV: funding acquisition, supervision, formal analysis.

Editors: José Marcio Calixto, Guilherme Aris Parsekian.